ON THE SOLUTE TRANSPORT IN AN AQUIFER-AQUITARD SYSTEM

A Dissertation

by

AIGUO BIAN

Submitted to the Office of Graduate Studies of
Texas A&M University
in partial fulfillment of the requirements for the degree of

DOCTOR OF PHILOSOPHY

May 2007

Major Subject: Geology

ON THE SOLUTE TRANSPORT IN AN AQUIFER-AQUITARD SYSTEM

A Dissertation

by

AIGUO BIAN

Submitted to the Office of Graduate Studies of
Texas A&M University
in partial fulfillment of the requirements for the degree of

DOCTOR OF PHILOSOPHY

Approved by:

Chair of Committee，	Hongbin Zhan
Committee Members,	Christopher C. Mathewson
	Yalchin Efendiev
	Binayak Mohanty
	Clyde Munster
Head of Department,	John Spang

May 2007

Major Subject: Geology

ABSTRACT

On the Solute Transport in an Aquifer-Aquitard System.

(May 2007)

Aiguo Bian, B.S., Beijing University, China

Chair of Advisory Committee: Dr. Hongbin Zhan

This dissertation is composed of five chapters and three major contributions are presented in Chapter II, III and IV.

Chapter I provided a review of studies on solute transport in aquifer-aquitard system. If the aquitard is considered, two categories of methods address the diffusive flux between the aquifer and aquitard: the old method treats the diffusive flux as a volumetric source in the governing equation of the solute transport in the aquifer; the new method treats the aquifer-aquitard boundary as a strict physical boundary with the requirement of continuity of solute concentration and the vertical flux. The new method is adopted throughout this study.

In Chapter II, a review of numerical techniques on Inverse Laplace Transform is provided. By careful comparison between several popular algorithms, the multiple precision Stehfest algorithm is chosen as the method to inverse out solutions on solute transport in Laplace domain throughout this dissertation.

In Chapter III, solutions were obtained for two dimensional solute transport in an aquifer-aquitard system with a divergent radial flow field, which can treat different types

of solute input function and advection, longitudinal and transverse dispersion in the aquifer, vertical diffusion in the aquitard, retardation and radioactive decay in the aquifer and aquitard are taken into account. Mass exchange via diffusion between the aquifer and aquitard are investigated. The effects of hydrologic properties of the aquitard on solute transport are analyzed. Comparisons were made between the results from this study and those from previous studies. The diffusion along the aquifer-aquitard boundary was treated as a volumetric source term, and proved these solutions yield more accurate solute concentration, while those from previous studies tend to overestimate solute concentration in the aquitard, and underestimate the concentration in the aquifer.

In Chapter IV, solutions were derived for the transport of radioactive isotopes in an aquifer-aquitard system with regional flow field. This study focused on the effects of different solute transport processes on the results of groundwater age dating using radiometric techniques.

Chapter V summarized the remaining problems in this study and directions for future researches.

DEDICATION

To my beloved parents and parents-in-law, my wife, Qiufeng Hao,

and my son, Benjamin Bian.

ACKNOWLEDGMENTS

I would like to give my thanks to my graduate advisor, Dr. Hongbin Zhan, for his support: philosophically, academically and financially. During my four years of graduate studies under him, he taught me a lot, both in how to do scientific research and how to succeed as a human being.

I appreciate all the excellent advice from the five members of my advisory committee. They did not push me too much, but whenever I needed them, they were not far away from me. Whenever I had a question, they had the answer available. I believe I will benefit from their direction and suggestions forever.

I would like to give thanks to my family. I haven't visited my mother during my four years as a doctoral student. I worry I am not a good son because of this, but I never heard her complain. My wife is another person who sacrificed a lot for me. She had a good job in Beijing, China before she married me and joined me in Texas. Here she suffered from things like the extremely hot summer in Texas, staying in a small apartment, cooking food for the whole family, living with a minimal income from my assistantships and studying basic English. In all kinds of circumstances, good or bad, happy or sad, I will never feel lonely simply because of her. Our son, Benjamin Bian, was born during my graduate studies. We had to send him back to China when he was 9 months old because we did not have sufficient time to care for him. I really feel sorry about that even though I did not feel I had any other choices. My parents-in-law have taken care of him for almost one year. Here I would like to express my thanks to them for their time and loving care.

Many thanks go to Dongmin Sun and Xianghe Zhou. Mrs. Sun graduated last

summer. Before her graduation, she and her husband gave us innumerable help. I also benefited from the discussions with Mrs. Sun on my research.

Finally, I thank the National Science Foundation of China (#50428907) and the CONACYT-TAMU Collaborative Research Program for the financial support for this study.

TABLE OF CONTENTS

Page

Page

LIST OF TABLES

LIST OF FIGURES

FIGURE Page

CHAPTER I

GENERAL INTRODUCTION

Although 75% of the earth's surface is covered water, about 97% of the total water is salty and not readily drinkable. Out of the remained 3% of fresh water, 2/3 is locked in the form of ice sheet or glaciers. In a word, only about 1% of the total water is available to human beings. Water crisis is forecasted in the near future [*Gleick*, 1993], it is partially because of the ever increasing water demanding with the ever increasing population in the world, and partially because a large portion of water resources, especially the surface water bodies, has been contaminated. Once the contaminants enter the drink water systems, they will post great threat onto the health of local communities. Overdraw of groundwater is commonly practiced in large cities in order to provide sufficient water supply. As a consequence, the groundwater level is lowered substantially. Lower groundwater level does not only cause more difficult to pump groundwater out, but also land subsidence and land degradation. People are polluting water body by their carelessness or unawareness, for example, abuse of pesticide, fertilizer and agricultural chemicals, leakage of underground gas tank and the like. Based on the USEPA 305(b) Report [*USEPA,* 1998], 37 states reported potential sources of groundwater contamination.

This dissertation follows the style of *Water Resources Research*.

To understand the mechanics that controls the solute transport in groundwater system, scientists developed numerous analytical and numerical modeling tools model water flow and solute transport in the aquifer. The success of modeling depends strongly on the quality of input aquifer characteristic parameters, such as porosity, conductivity, and dispersivity. These characteristic properties can be collect by tracer tests, subsurface borehole investigation, isotopes, or geophysical method. Geophysics methods are capable to collect large amount data in big areas but the results are limited by the resolution, detection range and parameterization problems [*Hubbard and Rubin*, 2000]. Pumping tests and tracer tests are most commonly used for site characterization. Tracer tests can be either under natural hydraulic gradient or forced hydraulic gradient condition, and their configuration can be either divergent or convergent, and the tracer used can be both reactive and non-reactive [*Ptak et al.*, 2004], depending on the different testing purposes. Numerous tracer tests have been conducted including Borden, Ontario, Canada; Otis Air Force Base, Cape Cod, Massachusetts; Hanford, Washington; Mobile, Alabama; etc. The results of carefully designed tracer tests can be interpreted either by comparing with some existing analytical solutions or by the method of spatial moments [*Freyberg*, 1986] to yield dispersivity estimations. For deep aquifer, artificial tracer tests are very difficult to conduct, so scientists use isotopes as a natural occurring tracer [*Plummer et al.*, 1998].

Because the heterogeneity nature, groundwater system can be divided into high conductivity layers termed as aquifer and low conductivity layers termed as aquitard.

Small scale heterogeneity such as clay lenses in high permeability rocks are commonly observed [e.g. *Pinder,* 2002, Figure 1.27]. Enormous amount of experimental, analytical, and numerical studies have been conducted on solute transport in porous media. But most of these studies focus on the role of aquifers as the avenue of solute advection, dispersion, diffusion, as well as reaction. The role of aquitards adjacent to the main aquifers on solute transport is often ignored and the aquitard-aquifer interface is often treated as a no-flux boundary for transport [*Bear*, 1972; *Domenico and Schwartz,* 1998; *Fetter,* 1999]. Some takes diffusion into account, but treats diffusion flux as a volumetric source/sink term in the Advection-Dispersion Equation (ADE) for the aquifer. Assuming ideal mixing of solute along the vertical axis, the vertical averaged concentration is used in ADE instead of actual concentration. By these simplifications and assumptions, these researchers were able to simulate solute transport in an aquifer-aquitard system using one-dimensional model.

Aquitards consist of low permeability materials such as silt and clay so they are poor in transmit water, but the total porosities of silt and clay are comparable, sometimes even larger than those of sands, so aquitards are well capable of storing water and solute. Considering solute transport in an aquifer-aquitard system, the molecular diffusion will drive solute into the aquitard once a vertical concentration gradient exists along the aquifer and aquitard boundary.

The interests of study the roles of diffusion along aquifer-aquitard boundary started from the study of fractured rocks. Hydrologists concerned about the fractures in grantitic rocks as a potential leakage path for the nuclear wastes when the nuclear water

disposal site is proposed in Yucca Mountain, NV. Simple analytical models [*Tang et al.*, 1981; *Sudicky and Frind*, 1982, 1984; *Fujikawa and Fukui,* 1990] treated the rock matrix-fracture system in a similar way as an aquitard-aquifer system. Many studies in fractured media have shown that matrix diffusion is the primary factor for retarding the contaminants in the fractures [e.g. *Neretnieks,* 1980; *Rasmuson and Neretnieks,* 1981; *Neretnieks et al.*, 1982; *Moreno et al.*, 1985]. The differences between a fracture-matrix system and aquifer-aquitard system lie in that the aperture of the fracture is much smaller than the aquifer thickness and the flow velocity in the fracture is often much greater than that in the aquifer under the same hydraulic gradient. Although the value of molecular diffusion in the aquitard is often much smaller than the hydrodynamic dispersion in the aquifer, its effect on solute transport across the aquitard-aquifer boundary could be significant, as indicated in previous study of previous studies layered porous media [*Sudicky et al.*, 1985; *Starr et al.*, 1985; *Tang and Aral*, 1992a, b]. Laboratory experiments of *Sudicky et al.* [1985], *Starr et al.* [1985], *Young and Ball* [1998] and numerous field aquifer studies such as *Johnson et al.* [1989], *Ball et al.* [1997a, b], *Liu and Ball* [1999], *Hendry et al.* [2003], *Hunkeler et al.* [2004], *Parker et al.* [2004] and others provided evidences of aquitard diffusion as an important controlling factor on solute transport in porous media. *Liu and Ball* [1999] provided a concentration profile crossing an aquifer and two covering aquitards. Both aquitards contain significant amount of TCE and PCE. Back diffusion from the aquitard to the aquifer after the passing of the solute front is the main cause of the tailing effect

observed in the aquifer and has caused great disadvantage for removing contaminants from the aquifer [*Liu and Ball*, 2002].

Most of the aforementioned analytical studies either ignored the aquitard or treated the aquitard diffusion as a volumetric source. *Sudicky et al.* [1985] have realized that in real aquifers, the transverse mixing is probably not always rapid enough to warrant mixing fast enough to use a thickness-averaged approach. This is not hard to understand. Recall the Leibnitz's rule for differentiation of an integral, one can easily prove that using thickness averaged value is problematic once the concentration gradient along vertical direction can not be neglect. Consider a standard 2-D ADE equation [Bear, 1972, Freeze and Cherry, 1979]:

$$\frac{\partial C}{\partial t} + v\frac{\partial C}{\partial x} - D_x\frac{\partial^2 C}{\partial x^2} - D_z\frac{\partial^2 C}{\partial z^2} = 0 \tag{1-1}$$

One can integrate (1-1) along vertical direction:

$$\int_a^b \left(\frac{\partial C}{\partial t} + v\frac{\partial C}{\partial x} - D_x\frac{\partial^2 C}{\partial x^2} - D_z\frac{\partial^2 C}{\partial z^2}\right)dz = 0 \tag{1-2}$$

Notice that the upper and lower boundary is constant, so by Leibnitz's rule (1-2) equals:

$$\frac{\partial}{\partial t}\left(\int_a^b C dz\right) + v\frac{\partial}{\partial x}\left(\int_a^b C dz\right) - D_x\frac{\partial^2}{\partial x^2}\left(\int_a^b C dz\right) - D_z\left(\frac{\partial C}{\partial z}\Big|_b - \frac{\partial C}{\partial z}\Big|_a\right) = 0 \tag{1-3}$$

Therefore, they proposed an alternative method of treating the diffusive flux at the aquitard-aquifer interface as a boundary condition rather than a source term in the governing equation of transport in the aquifer.

Zhan et al. [2006] proposed a new analytical approach. They took into account both the longitudinal and vertical dispersions in the aquifer and the transport in the aquifer was treated as a two-dimensional problem. They ended up solving the two-dimensional transport in the aquifer and one-dimensional diffusion in the aquitard simultaneously for a fully penetrating, horizontally infinite source without using the averaged approximation employed such as by *Sudicky et al.* [1985], *Chen* [1985], *Tang and Aral* [1992a, b], and others. The aquifer-aquitard contact is treated as a physical boundary, requiring continuity of both solute concentration and vertical flux across the boundary. The approach satisfies the mass balance requirement rigorously in both the aquifer and aquitard.

The purpose of this study is to extend the mathematical model by *Zhan et al.* [2006] and provide some useful application. Chapter III will provide the extension to cylindrical coordinate system. And this model is well suitable of study divergent tracer test. Chapter IV provides another extension by including radioactive decay and retardation, with the application in groundwater age dating.

CHAPTER II

NUMERICAL INVERSION OF LAPLACE TRANSFORMATION

Laplace transform is very useful in solving partial differential equations. By conducting of Laplace transform, one of the variables is dropped out, so the original partial differential equation reduced to a relatively simpler differential equation. The Laplace transform of a function *f(t), t* $\geq$ *0* is defined as:

$$F(p) = \int_0^\infty e^{-pt} f(t) dt \tag{2-1}$$

F(p) is the Laplace transform of *f(t)*. Function *f(t)* is a piecewise continuous real valued function of the real variable t (*t* $\geq$ *0),* and of exponential order, which means there exists a T, once t > T, then:

$$\left| f(t) \right| < Me^{at} \tag{2-2}$$

where M, a, T are all positive constants. If these requirement are fulfilled, then the Laplace transform of *f(t)* exists in he half plane of the complex variable *p* for which the real part of p is greater than some fixed value p_0 or R(p) $\geq p_0$.

Inversing Laplace transform will yield function *f(t):*

$$f(t) = \frac{1}{2\pi i} \int_{a-i\infty}^{a+i\infty} e^{pt} F(p) dp \tag{2-3}$$

where $\alpha > p_0$.

There are numerous numerical methods and computer codes for numerical inversion of Laplace transform available in the literature [see *Valko and Vajda,* 2002 and

the references thereafter]. Among them the most popular methods are Talbot's method [*Talbot* 1979], De Hoog's Method [*de Hoog et al.* 1982] and Stehfest's method [*Stehfest* [1970].

Talbot's algorithm is based on calculation of integral (2-3) using numerical quadrature along changed contour line. To use this method, the user is required to provide all the locations of singularities, and values of parameters that will be used to define the contour line [*Murli and Rizzarli*, 1990].

De Hoog's algorithm is based on accelerating the convergence of the Fourier series obtained from the inversion integral (Eqs. 2-3) using a trapezoidal rule. Acceleration is achieved by using the Pade approximation and quotient-difference algorithm. This method is very convenient to use, and is considered to be the most accurate method in many cases [see Figure 2-1].

Stehfest's algorithm is based on the Gaver's method [*Gaver,* 1966]. They considered the expectation of *f(t)* with respect of a certain probability density function. They found out that the expectation converges to *f(t)*. The final inversion formula they used is as follow:

$$f(t) = \frac{\ln 2}{T} \sum_{i=1}^{N} V_i F(\frac{\ln 2}{T} i) \qquad (2\text{-}4)$$

Where N must be an even integer. V_i depends on N only and is defined as:

$$V_i = (-1)^{N/2+i} \sum_{k=\frac{i+1}{2}}^{Min(i,N/2)} \frac{k^{N/2+1}(2k)!}{(N/2-k)!k!(k-1)!(i-k)!(2k-i)!} \qquad (2\text{-}5)$$

This method is very easy to program and use, but is criticized for poor accuracy

[*Tseng and Lee*, 1998].

Algorithms by *Talbot* [1979] and *de Hoog et al.* [1982] are not suitable to inverse solutions derived in this paper, because both of them need to calculate Laplace domain functions with complex variables. All of our solutions derived in chapter III and IV involve frequency ω_n and/or μ_n. For example, in chapter III, ω_n in Section 3.2.2 is given by Eqs. (A-9) in APPENDIX A, the roots of equation $\omega_n \tan(\omega_n) = k_2 r\sqrt{k_3 + k_1 p}$. The performance of this equation with complex *p* is not well understood. The *Stehfest* [1970] method only requires calculate real variable functions and has been used successfully by several hydrologists in similar problems [*Moench and Ogata*, 1981; *Moench*, 1991, *Valko and Valja*, 2002]. It is known for long time that accuracy of the Stehfest algorithm can be improved if one uses bigger N [*Stehfest,* 1972], but the improvement is limited by the number of digits used by the computer to represent float numbers. In a fixed precision calculation environment, the improvement of accuracy by using bigger number of N will soon be diminished by round off error. *Valkó and Vajda* [2002] and *Valkó and Abate* [2004] improved the Stehfest algorithm by conducting numerical inversion in a multiple precision environment such as FORTRAN and Mathematica. By using Mathematica or FORTRAN, one can increase the number of digits of float numbers instead of using fixed precision software such as Matlab. As a consequence, one can use bigger N in the Stehfest method. Using more significant digits also rewarded by faster rate of convergence. The reason is that Stehfest found the optimal coefficients in the sense that it eliminates N-1 members of the Post-Widder formula [*Frolov and Kitaev,* 1998]. In this way better accuracy is achieved.

Figure 2-1 shows the comparison of inversing results of function *f(t) = sin(t),* using traditional Stehfest method calculated in Matlab and multi-precision Stehfest method calculated in Mathematica. Its Laplace transform is $F(s) = 1/(s^2+1)$. Multi-precision Stehfest yields results almost the same as exact value. As for traditional Stehfest method, N = 24 is the best inversing result one can get, but it starts to drifting away from exact value when t approaches 2π. When we continue to increase N in Stehfest algorithm, the results began to oscillate in positive and negative values, as described by [*Tseng and Lee,* 1998].

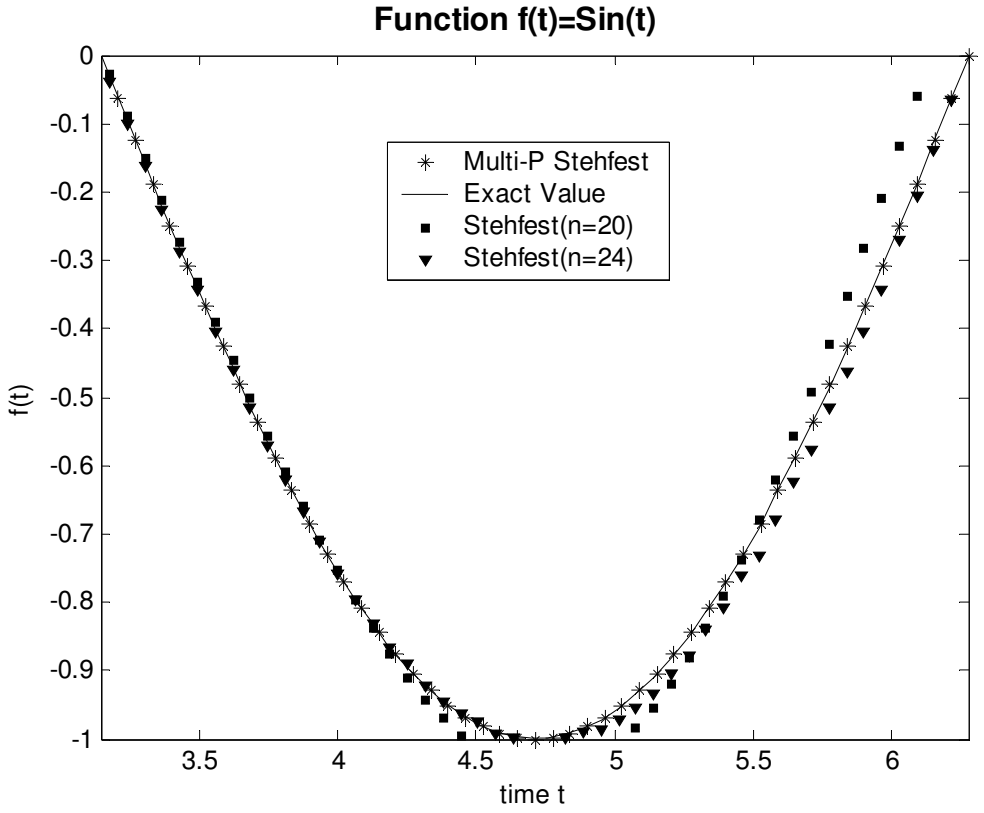

Figure 2-1. Plot shown exact solution compared with numerical Laplace transform inversion using different methods.

Figure 2-1 and some other comparison experiments proved the effectiveness and accuracy of the multiple precision Stehfest algorithm in most cases we tried, so we will use it as the default method to invert Laplace transform, unless otherwise pointed out. Most of the calculations in this dissertation are done in Mathematica 4.0, while diagrams are plot in Matlab 6.6.1 to take advantage of the powerful plot functions of Matlab. The Mathematica scripts are available from the author upon requests.

CHAPTER III

SOLUTE TRANSPORT IN A RADIAL FLOW AQUITARD-AQUIFER SYSTEM

Aquitards are important layers for protecting clean water in the adjacent aquifers. Contaminants traveling in the aquifer can diffuse into the adjacent aquitards and in turn the contaminated aquitard may become contaminant sources of another aquifer layer. But diffusion process is often ignored by most of present conceptual models. A few studies have considered aquitard diffusion, but they have adopted a methodology used in fracture-matrix systems by treating diffusing flux across the aquitard-aquifer interface as a volumetric source/sink term in the governing equation of transport in the aquifer. It has been recently noticed that this simplification does not satisfy the mass conservation requirement rigorously [*Sun & Zhan*, 2006] and its accuracy is unclear. The purpose of this paper is to present our work on solute transport in a divergent flow field such as injection tracer test. We focused on the aquitard control on solute transport through aquifer-aquitard system via diffusion. Diffusion along the aquifer-aquitard interface is treated as a boundary condition as it should be. This approach allows us to maintain the continuity of concentration and vertical solute flux at the aquitard-aquifer interface. Comparisons show our new solutions yield more realistic results in terms of vertical concentration profile cross the aquifer-aquitard boundary, and vertical averaged concentration in the aquifer.

3.1. Introduction

The roles of aquitards in solute transport in aquifer-aquitard systems are often ignored. The aquitard-aquifer interfaces are often treated as no-flux boundaries for solute transport in their work [*Bear*, 1972; *Domenico and Schwartz*, 1998; *Fetter*, 1999]. Although aquitards are low in permeability because of their small effective porosity, the total porosity of aquitards can be even larger than that of the aquifers. So aquitards are well capable to store large amount of solute particles. Moreover, aquitard composed by clay usually bear negative electricity, which will enable it to adsorb positive ions. After the solute front pass through the aquifer, back diffusion from the aquitard to the aquifer is the primary cause of the tailing effect observed in the aquifer, which has caused great difficulty for contaminants remediation [*Liu and Ball*, 2002]. Many studies in fractured media have shown that matrix diffusion is the primary factor for retarding the contaminants in the fractures [e.g. *Neretnieks*, 1980; *Rasmuson and Neretnieks*, 1981; *Neretnieks et al.*, 1982; *Moreno et al.*, 1985]. Evidences of aquitard diffusion as an important controlling factor on solute transport in porous media have been shown in the laboratory experiments of *Sudicky et al.* [1985], *Starr et al.* [1985], *Young and Ball* [1998], and in numerous field aquifer studies such as *Johnson et al.* [1989], *Ball et al.* [1997a, b], *Liu and Ball* [1999], *Hendry et al.* [2003], *Hunkeler et al.* [2004], *Parker et al.* [2004] and others.

A common methodology dealing with diffusion from aquifer to the aquitards is to treat the diffusion flux as a volumetric source/sink term in the governing equation. This treatment substantially simplified the mathematical modeling, and works well in

fracture/matrix system, but may not reflect the true physics occurred in the aquitard-aquifer system and may be problematic in aquifer-aquitard system. Another methodology proposed by *Sun and Zhan* [2006] in their study of flow to a horizontal well in an aquifer-aquitard system is to treat the diffusion along the aquifer-aquitard interface as a boundary condition. Continuity of hydraulic head and vertical flux are used to close the problem. Their study shows that the differences between results from the two methodologies can be very large. One assumption of treating diffusion as source/sink term is that mixing along the vertical direction should be very rapid so that a vertical averaged concentration can be used. This assumption may hold in fracture/matrix system, because the fracture aperture is usually very thin and flow rates in fractures are generally fast. In aquifer-aquitard system, relative low flow rate in the aquifer compared with that in the fracture, relative thicker aquifer layers may break the assumption. *Sudicky et al.* [1985] and *Starr et al.* [1985] have investigated the aquitard diffusion effect in an artificial sandy aquifer whose thickness is about 0.02 to 0.03 meters. In this case the quick vertical mixing can be easily achieved. *Chen* [1985] and *Tang and Aral* [1992a, 1992b] have adopted this source/sink term approach to study dispersion-diffusion in an aquitard-aquifer system with radial and uniform flows, respectively. The same approximation has been broadly adopted in studying matrix diffusion in fractured media [*Neretnieks*, 1980; *Rasmuson and Neretnieks*, 1981; *Tang et al.*, 1981; *Neretnieks et al.*, 1982; *Sudicky and Frind*, 1982, 1984; *Fujikawa and Fukui*, 1990].

When it comes to injection well tracer tests or deep waste water injection, one will have to deal with solute transport in a divergent flow field. Analytical study of solute transport in a divergent flow field can be traced back to 1960s' [*Hoopes and Harleman*, 1967; *Moench and Ogata*, 1981; *Chen*, 1985, 1987; *Hsieh*, 1986]. Most of these studies focusing on solute transport in the aquifer. *Chen* [1985] addressed the role of aquitard diffusion, but a volumetric source/term approach is adopted in his study. In this study, we will treat diffusive transport at the aquitard-aquifer interface as a boundary condition rather than a source/sink term in the transport governing equation, and so ensure the continuity of concentration and mass flux across the aquitard-aquifer interface. Therefore, this approach satisfies the mass balance requirement rigorously in both the aquifer and aquitard. The purpose of this paper is to illustrate the merits of the new approach and demonstrate the importance of the aquitard effect on solute transport.

3.2. Conceptual and Mathematical Models

3.2.1. Conceptual model

The system investigated is an injection well fully penetrating a homogeneous and horizontally isotropic aquifer with constant longitudinal and vertical dispersivity. The aquifer is bounded by either two aquitards from top and bottom or by an aquitard from top and bedrock from bottom. The aquitard-aquifer and the bedrock-aquifer boundaries are assumed to be horizontal, and the aquifer, the aquitards, and the bedrock extend horizontally to infinity. The aquitards are homogeneous and sufficiently thick so that solute diffusion is not affected by their thicknesses. Figures 1A-1C shows the schematic diagrams of three cases that will be investigated. They are an aquifer bounded by

identical upper and lower aquitards, an aquifer bounded by an upper aquitard and lower bedrock, and an aquifer bounded by different upper and lower aquitards, respectively. The hydraulic conductivity of the aquitard is assumed to be a few orders of magnitude smaller than that of the aquifer, thus the vertical flow in the aquitard is negligible. Steady-state horizontal flow is established in the aquifer. *Liu & Ball* (1999) measured the pressure differences in the aquitard along the vertical direction, and concluded the differences are so small that the vertical flow can be safely neglected.

The coordinate system is set as follows. The *r*- and *z*- axes are along the horizontal and vertical directions, respectively with the origin at the left boundary. Because of the symmetry of the geometry in Figure 3-1A, the origin is set at the middle of the aquifer layer, while the origins are set at the aquifer bottom in Figure 3-1B and Figure 3-1C.

Advection, longitudinal, and vertical dispersions are considered for transport in the aquifer. Vertical diffusion is considered in the aquitard. First-order kinetic reaction is considered in both aquifer and aquitard to deal with radioactive decay, or biodegradation or hydrolysis. It is assumed that the aquifer and aquitard are free of solutes at the start of transport. Depending on the different design of tracer tests and the actual field conditions, the boundary condition can vary significantly. The mathematic model presented here is able to deal with different injection scenario, from plus injecting, to periodical injecting, to constant injecting, from fully penetrating injecting to partially penetrating injecting, once the injecting can be described by a function of time and vertical coordinate. Based on the conceptual model, the following mathematical models are established.

3.2.2. Solute transport in an aquifer bounded by identical upper and lower aquitards

The governing equations [Bear, 1972, Freeze and Cherry, 1979] and initial and boundary conditions for both the aquifer and aquitard of this case are as follows. For the aquifer,

$$\frac{\partial C}{\partial t} = \frac{1}{r}\frac{\partial}{\partial r}\left(rD_r \frac{\partial C}{\partial r} \right) + D_z \frac{\partial^2 C}{\partial z^2} - v\frac{\partial C}{\partial r} - \lambda C \,, \tag{3-1}$$

$$C(r = r_0, z, t) = f(z,t) \,, \tag{3-2}$$

$$C(r = +\infty, z, t) = 0 \,, \tag{3-3}$$

$$\frac{\partial C(r, z = 0, t)}{\partial z} = 0 \,, \tag{3-4}$$

$$C(r, z, t = 0) = 0 \,, \text{ for } r > r_0, \tag{3-5}$$

And for the aquitard,

$$\frac{\partial C_1}{\partial t} = D_1 \frac{\partial^2 C_1}{\partial z^2} - \lambda C_1 \,, \tag{3-6}$$

$$C_1(r, z = B, t) = C(r, z = B, t) \,, \tag{3-7}$$

$$\theta_1 D_1 \frac{\partial C_1(r, z = B, t)}{\partial z} = \theta D_z \frac{\partial C(x, z = B, t)}{\partial z} \,, \tag{3-8}$$

$$C_1(r, z = +\infty, t) = 0 \,, \tag{3-9}$$

$$C_1(r, z, t = 0) = 0 \,, \tag{3-10}$$

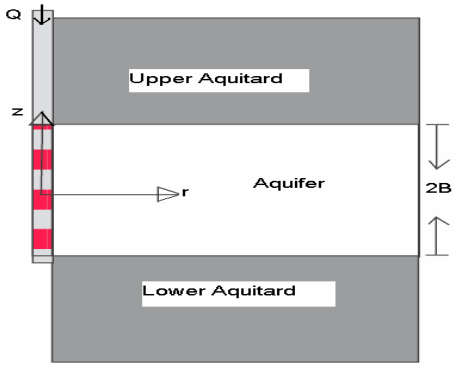

Figure 3-1A. Schematic diagram of an aquifer bounded by identical upper and lower aquitards.

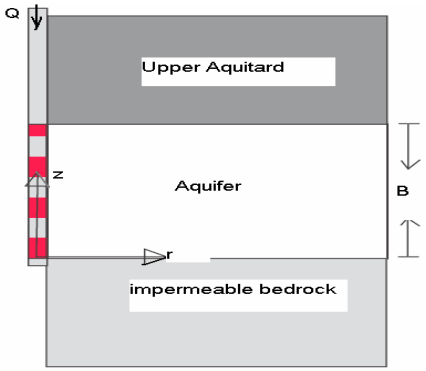

Figure 3-1B. Schematic diagram of an aquifer bounded by an aquitard from the top and bedrock at the bottom.

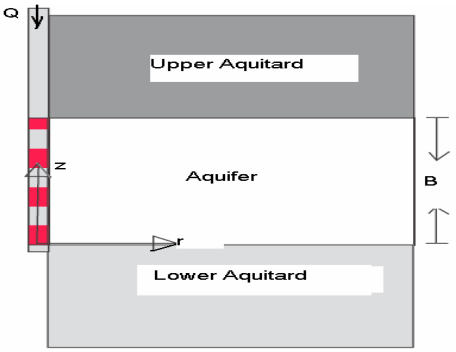

Figure 3-1C. Schematic diagram of an aquifer bounded by two different aquitards from the top and the bottom.

Where C and C_1 represent the residential concentrations in the aquifer and aquitard, respectively; θ_1 and θ are the porosities of the aquitard and aquifer, respectively; B is the half thickness of the aquifer; and t is time. v is the average pore velocity of groundwater flow in the aquifer; D_r and D_z are the longitudinal and vertical hydrodynamic dispersion coefficients respectively for the aquifer, and $D_r = \alpha_r v + D_0$, $D_z = \alpha_z v + D_0$, where α_r and α_z are the longitudinal and vertical dispersivities, respectively. D_0 is the molecular diffusion coefficient of the solute in pure water [*Bear*, 1972]. It is usually several orders of magnitude smaller than D_r and D_z, so generally can be safely omitted to facilitate mathematical manipulation. It is worthwhile to note that v is not a constant in case of divergent flow field of an injection tracer test. Instead it is a function of radial distance from the injection well $v = \frac{Q}{4\pi B\theta r}$, where Q is the injection rate of the injection well. D_1 is the effective molecular diffusion coefficient in the aquitard, $D_1 = \tau_1 D_0$, where τ_1 is tortuosity; λ is the decay constant for radioactive decay or reaction rate coefficient for biodegradation or hydrolysis.

Eqs. (3-1) is the advection-dispersion equation with first-order kinetic reaction of solute transport in a cylindrical coordinate system. Eqs. (3-2) is the boundary condition at the injection well. Notice here a general form function *f(z, t)* is used, which enables one to deal with different injection scenario, such as a constant injection, a pulse injection, a step function or multi-step function. Eqs. (3-3) is the boundary conditions at infinity in the aquifer. Eqs. (3-4) is the no mass flux condition at z=0 because of the mirror symmetry about z=0, and Eqs. (3-5) is the initial condition in the aquifer. Eqs. (3-

6) is the diffusion equation in the aquitard, Eqs. (3-7) and (3-8) are the continuity of concentration and mass flux at the upper aquitard-aquifer boundary at $z=B$, respectively. Eqs. (3-9) is the vertical boundary condition for a sufficiently thick aquitard, and Eqs. (3-10) is the initial condition in the aquitard.

Defining the following dimensionless terms:

$$r_D = \frac{r}{\alpha_r}\ ,\ z_D = \frac{z}{B}\ ,\ \beta = \frac{Q}{4\pi B\theta}\ ,\ t_D = \frac{\beta}{\alpha_r{}^2}t\ ,\ C_D = \frac{C}{C_0}\ ,\ C_{1D} = \frac{C_1}{C_0}\ ,\ k = \frac{\alpha_r\alpha_z}{B^2}\ ,$$
$$k_1 = \frac{B^2\beta}{\alpha_r{}^2 D_1},\ k_2 = \frac{\theta_1\alpha_r D_1}{\theta\alpha_z\beta},\ k_3 = \frac{\lambda B^2}{D_1} \qquad (3\text{-}11)$$

where subscript "*D*" represents the dimensionless term. The definitions of the dimensionless terms used in this chapter are also summarized in Table 3-1. After transforming above Eqs. (3-1) - (3-10) into dimensionless forms, applying the Laplace transform to the governing equations and boundary conditions will result in the following equation group. For the brevity of presentation, all the discussions in the rest of this paper are in dimensionless forms and the subscript "*D*" is removed.

$$rp\overline{C} = \frac{\partial^2\overline{C}}{\partial r^2} + k\frac{\partial^2\overline{C}}{\partial z^2} - \frac{\partial\overline{C}}{\partial r} - \lambda\overline{C}\ , \qquad (3\text{-}12)$$

$$\overline{C}(r = r_0, z, p) = F(z, p)\ , \qquad (3\text{-}13)$$

$$\overline{C}(r = +\infty, z, p) = 0\ , \qquad (3\text{-}14)$$

$$\frac{\partial\overline{C}(r, z = 0, p)}{\partial z} = 0\ , \qquad (3\text{-}15)$$

$$p\overline{C}_1 = \frac{1}{k_2}\frac{\partial^2\overline{C}_1}{\partial z^2} - k_3\overline{C}_1\ , \qquad (3\text{-}16)$$

$$\overline{C}_1(r, z = 1, p) = \overline{C}(r, z = 1, p)\ , \qquad (3\text{-}17)$$

$$\frac{\partial \overline{C}_1(r, z=1, p)}{\partial z} = \frac{1}{k_2}\frac{1}{r}\frac{\partial \overline{C}(r, z=1, p)}{\partial z}, \tag{3-18}$$

$$\overline{C}_1(r, z=+\infty, p) = 0, \tag{3-19}$$

where $\overline{C}$, $\overline{C}_1$ and *F(z, p)* are the Laplace transforms of *C*, C_1 and *f(z, t)*, respectively, and *p* is the Laplace transform parameter in respective to the dimensionless time.

The procedure of solving the above equation group of (3-12) - (3-19) is given in APPENDIX A. The derived solutions for $\overline{C}$ and $\overline{C}_1$ are:

$$\overline{C} = \sum_{n=0}^{\infty} G(F, p, \omega_n)\frac{A(r, p, \omega_n)}{A(r_0, p, \omega_n)}\cos(\omega_n z), \tag{3-20}$$

$$\overline{C}_1 = \sum_{n=0}^{\infty} G(F, p, \omega_n)\frac{A(r, p, \omega_n)}{A(r_0, p, \omega_n)}\cos(\omega_n)\exp\left[\sqrt{k_3 + k_1 p}(1-z)\right], \tag{3-21}$$

where the frequency ω_n is determined in (A-9) in APPENDIX A. $G(F, p, \omega_n)$ and $A(r, p, \omega_n)$ are defined as follow:

$$G(F, p, \omega_n) = \frac{4\omega_n \int_0^1 F(z, p)\cos(\omega_n z)dz}{2\omega_n + \sin(2\omega_n)}. \tag{3-22}$$

$$A(r, p, \omega_n) = e^{\frac{r}{2}} Ai[p^{-\frac{2}{3}}(rp + k\omega_n + \lambda + \frac{1}{4})] \tag{3-23}$$

where *Ai* is the Airy function which is the general solution of the differential equation:

$y'' - yz = 0.$ (3-24)

For more information on Airy function and its properties, the reader can refer to *Abramowitz and Stegun* (1972) or *Spanier and Oldham* (1987).

3.2.3. Solute transport in an aquifer bounded by an upper aquitard and lower bedrock

If the aquifer is bounded by an upper aquitard and lower bedrock which can be treated as a no-flux boundary for transport (Figure 3-1B), the solutions derived in section 3.2.2 can be easily modified to calculate the concentrations in the aquifer and aquitard. The central line of Figure 3-1A is a symmetric line, so it is actually a no vertical flux boundary, same as the bedrock in Figure 3-1B. If we redefine those dimensionless terms of Eq. (3-11) by replacing B with $2B$, then all the solutions derived in section 3.2.2 can be directly used to handle the case of Figure 3-1B.

3.2.4. Solute transport in an aquifer bounded by different upper and lower aquitards

In reality, the upper and lower aquitards usually have different physiochemical properties, because they are deposited at different geologic time and different environments, composed by different geological materials with different texture and structure. For instance, *Ball et al.* [1997a] has reported two different types of aquitards adjacent to the aquifer at Dover Air Force Base: an orange silty clay loam upper aquitard and a dark gray silt loam lower aquitard. So it is worth time to derive solutions for solute transport in an aquifer bounded by different upper and lower aquitards. Intuitively, the concentrations in the upper and lower aquitards may not be the same, so we denoted them as C_1 and C_2, respectively.

Using the coordinate system of Figure 3-1C, we assign D_{1u} and θ_{1u} for the effective molecular diffusion coefficient and porosity of the upper aquitard, respectively; and D_{1l} and θ_{1l} for the effective molecular diffusion coefficient and porosity of the lower aquitard, respectively. The origin of coordinate is set at the lower boundary of the aquifer, as shown in Figure 3-1C. Equations (3-6) – (3-10) still hold for the upper aquitard. The following equations are added to deal with the lower aquifer:

$$\frac{\partial C_2}{\partial t} = D_{1l}\frac{\partial^2 C_2}{\partial z^2} - \lambda C_2, \tag{3-25}$$

$$C_2(r, z = 0, t) = C(r, z = 0, t), \tag{3-26}$$

$$\theta_{1l} D_{1l}\frac{\partial C_2(r, z = 0, t)}{\partial z} = \theta D_z \frac{\partial C(x, z = 0, t)}{\partial z}, \tag{3-27}$$

$$C_2(r, z = +\infty, t) = 0, \tag{3-28}$$

$$C_2(r, z, t = 0) = 0, \tag{3-29}$$

Similar to equation (3-6) – (3-10), equation (3-24) is the governing equation in the lower aquitard with diffusion and first-order kinetic reaction, equation (3-25) and (3-26) state the continuity of concentration and vertical flux along the lower boundary of the aquifer, Equation (3-27) states solute will never reach the infinity and equation (3-28) states the lower aquitard is free of solute at time zero. The dimensionless terms of Eqs. (3-11) need to redefined using $2B$ to replace B. The upper and lower aquitards may differ in porosities (θ_1) and effective molecular diffusion coefficient (D_1). Subscripts u and l are used to denote these properties of the upper and lower aquitards, respectively. The constants k_1, k_2 and k_3 are the same as defined in Eqs. (3-11) except that the appropriate properties need to be used for upper and lower aquitards.

The details of mathematical modeling are shown in APPENDIX B. And the solutions of solute concentration in the aquifer (C), upper aquitard (C_1) and lower aquitard (C_2) in Laplace domain read:

$$\overline{C} = \sum_{n=0}^{\infty} \frac{A(r, p, \omega_n)}{A(r_0, p, \omega_n)} G(F, p, \omega_n, \mu_n) \cos(\omega_n z + \mu_n), \ 0 \le z \le 1. \tag{3-30}$$

$$\overline{C_1} = \sum_{n=0}^{\infty} \frac{A(r, p, \omega_n)}{A(r_0, p, \omega_n)} G(F, p, \omega_n, \mu_n) \cos(\omega_n + \mu_n) \exp\left[\sqrt{k_{3u} + k_{1u} p}(1 - z)\right], \ 1 \le z \le \infty. \tag{3-31}$$

$$\overline{C_2} = \sum_{n=0}^{\infty} \frac{A(r, p, \omega_n)}{A(r_0, p, \omega_n)} G(F, p, \omega_n, \mu_n) \cos(\mu_n) \exp\left[\sqrt{k_{3l} + k_{1l} p}\, z\right], \ -\infty \le z \le 0. \tag{3-32}$$

where frequencies ω_n and μ_n can be obtained from (B-11) and (B-12) of APPENDIX B. $A(r, p, \omega_n)$ is the same as defined in (3-23), but $G(F, p, \omega_n, \mu_n)$ differs from Eqs. (3-22):

$$G(F, p, \omega_n, \mu_n) = \frac{4\omega_n \int_0^1 F(z, p) \cos(\omega_n z + \mu_n) dz}{2\omega_n + \sin(2\omega_n + 2\mu_n) - \sin(2\mu_n)} \tag{3-33}$$

Now the solutions for the three cases with flexible inlet boundary conditions are derived in Laplace domain. It is difficult to inverse these Laplace transform analytically. Therefore, we will use numerical inverse Laplace transform to find the concentrations in real time domain.

3.3. Results Analysis

The goal of this paper is to demonstrate the importance of the roles of aquitards on solute transport in aquifer-aquitard systems and illustrate the merits of our new solutions over the previous studies. For the purpose of simplicity, we will not discuss here those cases such as first-order reaction, partial penetration source and complicate

input functions. Instead we will only consider a pulse injection or constant injection to illustrate the roles of aquitards on solute transport. The studies by *Moench and Ogata* [1981], *Hsieh* [1986] and *Chen* [1985] are chosen to compare with our new solutions. Solutions in *Moench and Ogata* [1981] and *Hsieh* [1986] are identical. They both neglected aquitard diffusion. *Chen* [1985] considered the aquitard diffusion but followed the volumetric source/term approach.

3.3.1. Comparison with previous studies with no diffusion

If the aquitard diffusions and first-order reaction are not considered, then the problem for a constant concentration at $r=r_0$ is identical to the problem discussed by *Moench and Ogata* [1981] and *Hsieh* [1986]. This is a special case of the general solution derived here. If we set the porosity of the aquitard to be 0, then no solute can diffuse into the aquitard, k_2 in Eqs. (A-9) equals 0, then $\omega_n = n\pi$, where n=0, 1, 2 ….. Thus the only non-zero A_n from Eqs. (A-11) is A_0. It is easy to verify Eqs. (3-20) will reduce to Eqs. (17) of *Hsieh* [1986]. The solution of *Hsieh* [1986] is modified to solve a Dirac delta function input in the injection well. The resulted break through curve at dimensionless distance 100 and 150 are presented in Figure 3-2 and 3-3 to compare the traditional Stehfest, multi-precision Stehfest and de Hoog algorithms. The de Hoog algorithm is believed to be accurate in most cases. Compare Figure 3-2 and 3-3, it is clear that the results using the multi-precision Stehfest method is identical with that of de Hoog. Traditional Stehfest algorithm underestimated the concentration and only works at short distance. This is consistent with the observation made by *Valko and Vajda* [2002].

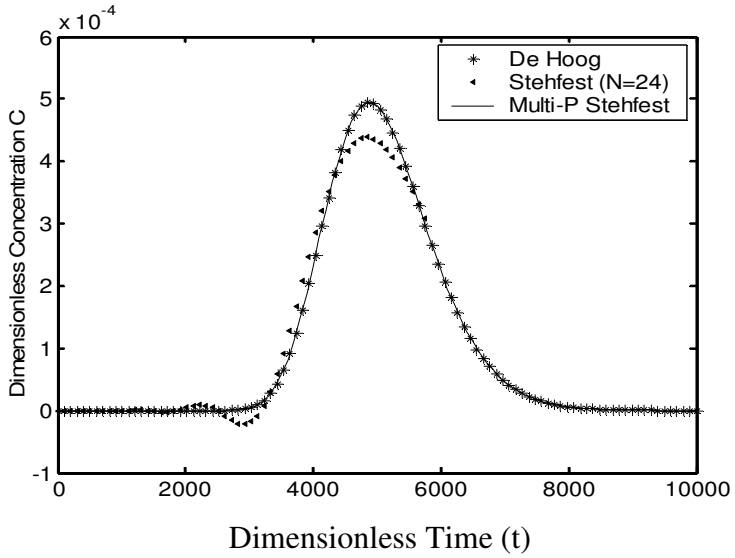

Figure 3-2. Results of Laplace transform inversion using different algorithms, (Dimensionless distance =100).

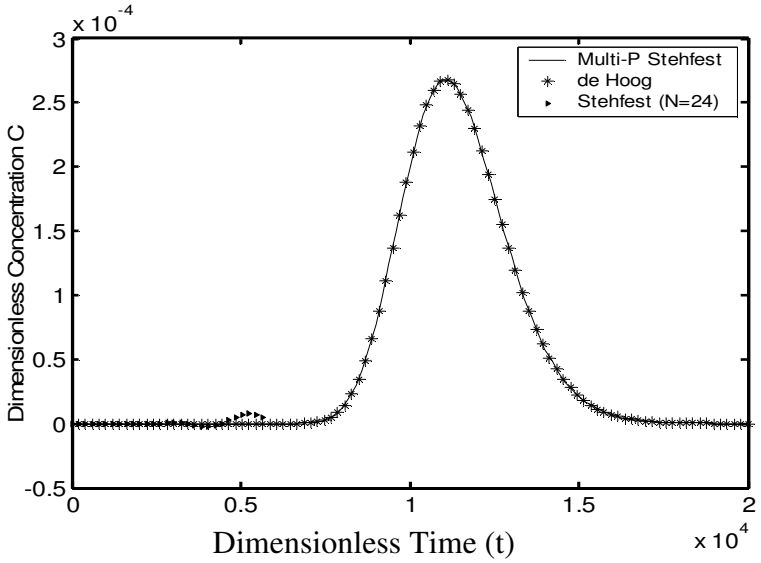

Figure 3-3. Results of Laplace transform inversion using different algorithms, (Dimensionless distance =150).

3.3.2. Comparison with approximation of aquitard diffusions with volumetric sources/sinks

Chen [1985] treated diffusion as a volumetric source/sink term in the governing equation of solute transport in the aquifer. Comparison of our solution with *Chen* [1985] is presented in Figures 3-4A and 3-4B. Figure 3-4A shows the concentration profile along vertical axis for different α_r value (α_r = 1, 5, 10). Result from *Hsieh* [1986] is also shown for reference. One can conclude that results from *Chen* [1985] are close to the vertical averaged values of our new solution, and both solutions give concentration lower than *Hsieh* [1986]. It makes sense because *Hsieh* [1986] did not consider diffusion from the aquifer to the aquitard. Figure 3-4B shows the concentration profile in the aquitard, predicted by our new solution and *Chen* [1985]. In all three α_r cases, *Chen* [1985] overestimated the concentration in the aquitard. This is not surprise because by taking vertical average of solute concentration in the aquifer, the concentration along the aquifer-aquitard boundary is overestimated, which means more solute particles will diffuse into the adjacent aquitard.

Another comparison between *Chen* [1985] and our solutions can be done in the following way: In most tracer tests, except those using multi-level samplers, samplers fully penetrating aquifer are used in the field. The measured concentration by this type of sampling is actually vertical averaged. So it is of interest to known the differences between our new solutions and those by *Chen* [1985] in calculating the vertical averaged concentration in both aquifer and aquitard. In order to compare the vertical averaged concentration predicted by *Chen* [1985] and our solution, we calculated the

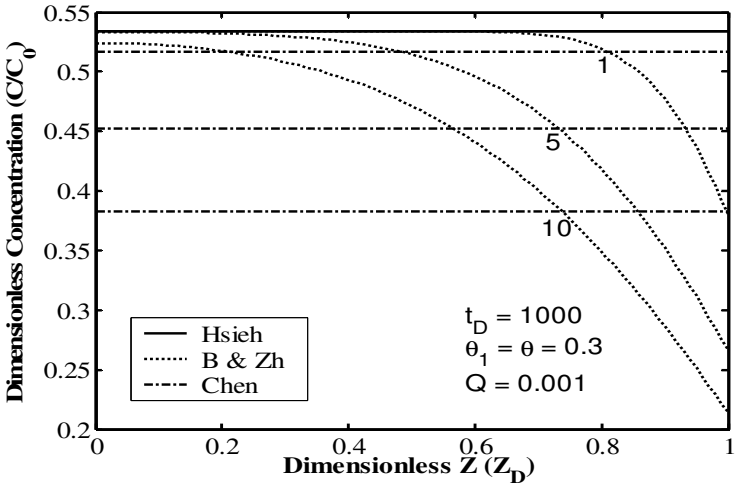

Figure 3-4A. Vertical concentration distribution profile in the aquifer for different dispersivities (α=1, 5, and 10).

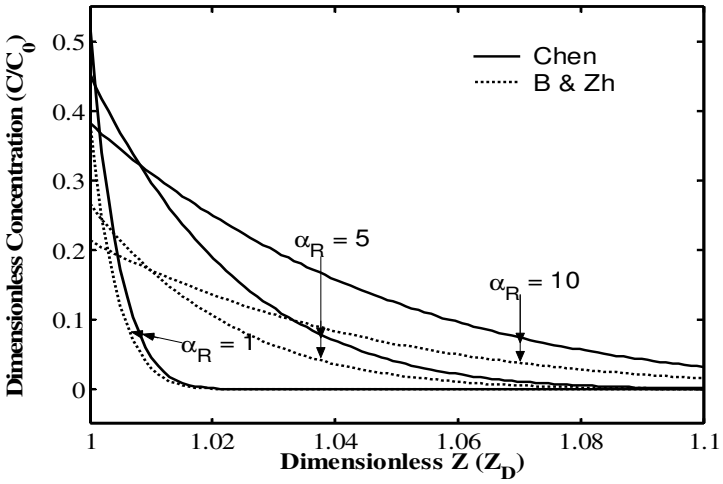

Figure 3-4B. Vertical concentration distribution profile in the aquitard for different dispersivities (α=1, 5, and 10).

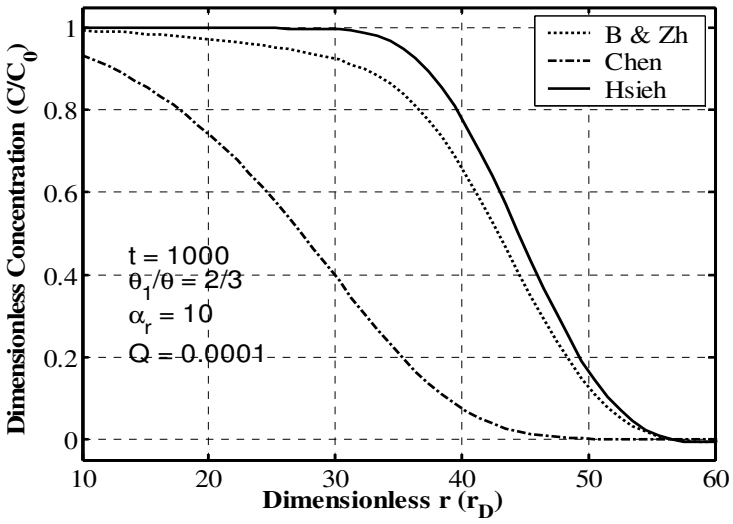

Figure 3-5. Vertical averaged concentration profile along radial axis.

concentrations at different points along the vertical line and then average these concentrations out. Some of this type of comparison is presented in Figure 3-5. Figure 3-5 shows the resulted vertical averaged concentration profile. We compared these two solutions using different parameter sets. All the comparisons conclude that the concentrations given by *Chen* [1985] are unanimously lower than those by our solutions, and our solutions are lower than *Hsieh* [1986]. This is because that *Hsieh* [1986] did not consider diffusion into the aquitard, while *Chen* [1985] overestimated the diffusion flux.

3.4. Summary and Conclusions

Solutions of solute transport in divergent flow field in an aquifer-aquitard system in Laplace domain are presented in this paper. Multi-precision Stehfest algorithm is

adopted to inverse these solutions into real time domain numerically. This algorithm provides more accurate inversing results compared with traditional Stehfest algorithm, and its accuracy is comparable with the de Hoog algorithm. The advantage of Stehfest algorithm lies in that it only requires function values in real domain, while de Hoog algorithm and Talbot algorithm, among others, require function values in complex domain.

Comparisons between our new solutions, *Moench and Ogata* [1981] and *Chen* [1985] show that our solutions provide better estimation of solute concentrations, both actual distributed concentrations and vertical averaged concentrations. *Moench and Ogata* [1981] overestimated the concentration in the aquifer because they neglected the diffusion flux into the aquitard, while *Chen* [1985] overestimated the concentration in the aquitard and underestimated that in the aquifer because they adopted the volumetric source/sink term approach.

The proposed solutions are able to deal with first-order kinetic reactions, so it can be used to investigate transportation of radioactive particles, biodegradation and hydrolysis in aquifer-aquitard systems. The input functions at the injection well are flexible, so it can be easily modified to analyze single injection well tracer test data.

Table 3-1: Definition of dimensionless terms used in Chapter III.

Dimensionless Term	Definition	Dimensionless Term	Definition
Dimensionless longitudinal coordinate	$r_D = \frac{r}{\alpha_r}$	Dimensionless vertical coordinator	$z_D = \frac{z}{B}$
Dimensionless Time	$t_D = \frac{\beta}{\alpha_r^{\,2}} t$	Dimensionless Concentration	$C_D = \frac{C}{C_0}$
Dimensionless Concentration in Upper Aquitard	$C_{1D} = \frac{C_1}{C_0}$	Dimensionless Concentration in lower Aquitard	$C_{2D} = \frac{C_2}{C_0}$
Dimensionless Injection Rate	$\beta = \frac{Q}{4\pi B\theta}$	Dimensionless Radioactive decay constant	$k_3 = \frac{\lambda B^2}{D_1}$
Dummy variables used in calculation	$k = \frac{\alpha_r \alpha_z}{B^2}$	Dummy variables used in calculation	$k_1 = \frac{B^2 \beta}{\alpha_r^{\,2} D_1}$
Dummy variables used in calculation	$k_2 = \frac{\theta_1 \alpha_r D_1}{\theta \alpha_z \beta}$		

,

CHAPTER IV

TRANSPORT OF RADIOACTIVE ISOTOPIC TRACER IN AN AQUITARD-AQUIFER SYSTEM: IMPLICATION OF GROUNDWATER DATING

This chapter is an extension of Dr. Hongbin Zhan's work [*Zhan et al.,* 2006] on two dimensional solute transport in an aquifer-aquitard system. Interpretation of groundwater age using radiometric dating methods based on so called piston flow model requires careful calibration the effects of dispersion, mixing, diffusion among other possible processes which will change the transport of radioactive tracers. Diffusion of radioactive nuclides from the main aquifer to the adjacent aquitards tends to dilute the radioactive tracer. Once the dilution effects are different for the radioactive and radiogenic isotopes, it will cause error in the dating results. In this chapter we present an analytical model of two dimensional transport of radioactive tracer in an aquifer-aquitard system, considering radioactive decay, hydrodynamic dispersion, retardation, and diffusion. Analysis of the solutions demonstrated the effect of diffusion from the aquifer to the aquitard can cause significant errors. The solution can be used to find the actual groundwater age from the measured radioactive tracer concentrations, or to estimate hydrologic parameters of the aquifer of interest.

4.1. Introduction

Radioactive tracers such as ^{3}H, ^{14}C, ^{36}Cl, among others, have been used successfully to date groundwater of different ages [*Kendall & McDonnell,* 1998]. Information of groundwater age can be used to find recharge rate [*Lehmann et al.,* 2003], differentiate different recharge sources [*Plummer et al.,* 1998], delineate the sea water intrusion zone [*Vengosh et al.,* 2002] and analysis flow path and refine a groundwater flow model [*Szabo et al.,* 1996]. Knowledge of groundwater age and its distribution in a deep aquifer is useful for assessing the dynamics of groundwater and planning its exploitation. *Kendall & McDonnell* [1998] provided excellent review of groundwater dating methods. Groundwater age is defined as the mean residence time of water particles. Interpretation groundwater age from radiometric dating method is generally based on the so-called piston flow model, which assumes the dating tracers are moving along a flow tube by advection only, so the mean residence time simply equals the transported distance divided by time. In isotropic, confined aquifers the water flow is laminar. Recharged young water move along a flow tube is suitable to apply the piston flow model. Hydrodynamic dispersion as long as mixing, diffusion can change the concentrations of the radioactive tracer and so change the apparent age by piston flow model. The roles of diffusion of solute from the aquifers to the adjacent aquitards are often ignored, and the aquitard-aquifer interfaces are often treated as no-flux boundaries for transport [*Bear*, 1972; *Domenico and Schwartz*, 1998; *Fetter*, 1999]. Although *Zlotnik and Zhan* [2005], from their study on aquitard effect on drawdown in water table aquifers, concluded that the water exchange between aquifer and aquitard played a minor

role at short or intermediate time, and its effects at long times can be neglected. But it does not necessarily mean that the diffusion of solute along aquitard-aquifer boundary is not important. Most aquitards consist of silt and clay. Their effective porosity and permeability are very small so they are not well capable in transmitting water, but they have large total porosity so they are well capable of storing water and solute. Although the value of molecular diffusion in the aquitard is often much smaller than the hydrodynamic dispersion in the aquifer, its effect on solute transport across the aquitard-aquifer boundary could be significant, as indicated from previous study of layered porous media [*Sudicky et al.*, 1985; *Starr et al.*, 1985; *Tang and Aral*, 1992a, 1992b], fractured media [e.g. *Neretnieks*, 1980; *Rasmuson and Neretnieks*, 1981; *Neretnieks et al.*, 1982; *Moreno et al.*, 1985], and laboratory experiments [*Sudicky et al.* [1985], *Starr et al.* [1985], *Young and Ball* [1998]] and field aquifer studies [*Johnson et al.* [1989], *Ball et al.* [1997a, b], *Liu and Ball* [1999], *Hendry et al.* [2003], *Hunkeler et al.* [2004], *Parker et al.* [2004] and others].

Several mechanics are worth consideration in interpretation of groundwater age data. In cases of the main aquifer is bounded by aquitards, if the aquitards have smaller tracer concentration than that of the aquifer, then diffusion of the radioactive tracers from the aquifer to the aquitard can dilute the concentration of radioactive isotopes [*Plummer et al.,* 1998; *Sudicky and Frind,* 1981]. Another possible diffusion mechanics is that once the water in the aquitard is much older than that in the aquifer, which is generally true, the older aquitard water can diffuse into the aquifer, so that an apparent age older than actual groundwater age will result. When ^{3}H and ^{3}He are used to date

groundwater, the diffusion coefficient of ^{3}He in air is much greater than that in water, so when possible direct contact of groundwater with air will cause ^{3}He loss, which will result in a younger apparent age. Some radioactive and radiogenic isotope pair have quite different diffusion coefficient, for example, the diffusion coefficient of ^{3}He is $5.74*10^{-5}$ cm^2/s at 10 ^{o}C [*Jahne et al.,* 1987] while that of ^{3}H is $1.57*10^{-5}$ cm^2/s at 10 ^{o}C [*Wang et al.,* 1952]. Effects of diffusion are magnified by retardation. Once solute particles entered the aquitards, adsorption and absorption of these particles onto the clay mineral surfaces will retard the solute transport. Most of the isotopes are bearing positive charges (except for Cl and some others), so they are easy to be trapped by the negative charged clay mineral surface.

Analysis of the effects of dispersion, mixing, diffusion and retardation can be done by numerical modeling [*Park et al.,* 2002], lumped parameter method [*Maloszewski et al.,* 2004], direct simulation approach using so called age mass [*Goode,* 1996; *Bethke and Johnson,* 2002] and analytical modeling. Most available analytical models are based on one dimension flow and transport model instead of two dimensional transport model, steady state analysis instead of transient analysis [*Sudicky and Frind,* 1981; *Atmadja et al.,* 2001] . In reality, a solute transport with radioactive decay, hydrodynamic dispersion, retardation and diffusion has to be treated at least as a 2-D problem [*Zhan et al.,* 2006].

In this study, we will extend the two dimensional analytical model developed by *Zhan et al.* [2006] to study radioactive tracer transport in an aquifer-aquitard system. The aquitard-aquifer interface is treated as a boundary of continuity of tracer concentration

and vertical flux to the conservation of mass. Radioactive decay, hydrodynamic dispersion, diffusion and retardation are considered. The effects of hydrodynamic dispersion and radioactive decay on groundwater age have been well understood [see chapter 7 and 8 of *Kendall and McDonnell,* 1998 and the references thereafter]. Therefore, this paper will focus more on the effect of diffusion and retardation on the transport of radiometric tracers. Mixing of difference sources of water and in-situ production of radiogenic isotopes will not be discussed.

4.2. Conceptual and Mathematical Models

4.2.1. Conceptual model

The system investigated is an aquifer bounded by two aquitards from top and bottom, or an aquifer bounded by an aquitard from top and bedrock from bottom. The aquitard-aquifer and the bedrock-aquifer boundaries are assumed to be horizontal. The aquifer is homogeneous and horizontally isotropic with constant longitudinal and vertical dispersivities. The aquitards are also homogeneous and sufficiently thick so that solute diffusion is not affected by their thicknesses. The aquifer, the aquitards, and the bedrock extend horizontally to infinity. Figures 4-1A to 4-1C show the schematic diagrams of three cases that will be investigated. They are an aquifer bounded by identical upper and lower aquitards, an aquifer bounded by an upper aquitard and lower bedrock, and an aquifer bounded by different upper and lower aquitards, respectively. The hydraulic conductivity of the aquitard is assumed to be a few orders of magnitude smaller than that of the aquifer, thus the vertical flow in the aquitard is negligible. *Zlotnik and Zhan* [2005] pointed out that the water exchange between the aquifer and

aquitard had minor effect on the drawdown of the water in the aquifer at short and intermediate times and the effect can be neglect at large time.

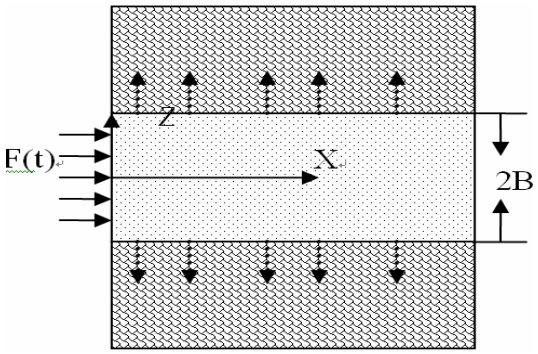

Figure 4-1A. Schematic diagram of an aquifer bounded from the top and bottom by identical aquitards.

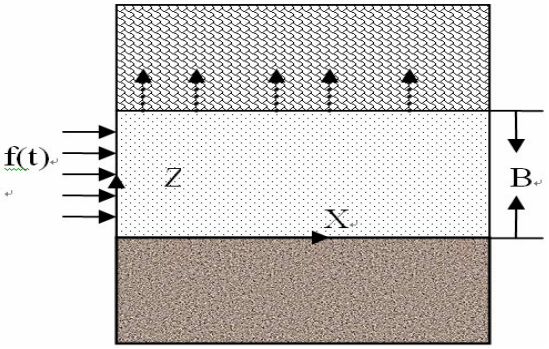

Figure 4-1B. Schematic diagram of an aquifer bounded by an aquitard from the top and the bedrock at the bottom.

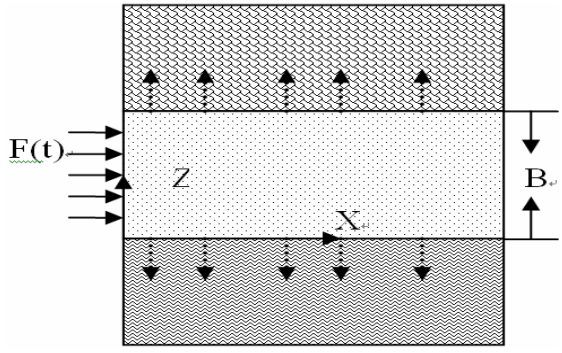

Figure 4-1C. Schematic diagram for an aquifer bounded from the top and bottom by different aquitards.

Husain et al. [1998] studied the long-term hydraulic gradient in the thick clayey aquitard in the Sarnia region, Ontario using one-dimensional solute transport model, and concluded that vertical profile of Cl- can be closely matched by diffusion with little or no vertical advection. Steady-state horizontal flow is established in the aquifer.

We set up the coordinate system as follows. The x- and z- axes are along the horizontal and vertical directions, respectively with the origin at the left boundary. Because of the symmetry of the geometry in Figure 4-1A, we choose the origin of the coordinate there at the middle elevation of the aquifer, and only consider the domain above the $z = 0$ axis. In Figures 4-1B and 4-1C, we choose the origins of the coordinate systems at the aquifer bottom.

Advection, longitudinal, and vertical dispersions are considered for transport in the aquifer. Vertical diffusion is considered in the aquitard. Radioactive decay and retardation are taking place in both aquifer and aquitard. It is assumed that the aquifer and aquitard are free from solutes at the start of transport. Based on the conceptual model, the following mathematical models are established.

4.2.2. Transport of radioactive isotope in an Aquifer-Aquitard system

We first consider the transport of radioactive isotope in an aquifer confined from the top and bottom by aquitards with same hydraulic characteristics, or in other words, identical aquitards. The schematic diagram is shown in Figure 4-1A. We consider the radioactive isotope was released at a constant concentration into the groundwater in the

aquifer at the time t = 0. This input can be described mathematically by $C = C_0$. Later we will show that our model is well capable to deal with complicated input functions, on condition that it is function of time only. Flow in the aquifer is horizontal and the water in the aquitard is treated as stagnant water. After the release, radioactive isotope will undergo horizontal advection, both horizontal and vertical dispersion in the aquifer. Once they enter the adjacent aquitard, the dominant transport process there is vertical diffusion. Radiogenic isotope will be produced from radioactive isotope through radioactive decay in both aquifer and aquitard. Another process we taking into account here is sorption and desorption at the mineral surface in both aquifer and aquitard. We assume that both the aquifer and aquitard have no background concentration of these isotopes. We also assume that there are no other sources of these isotopes in both aquifer and aquitard, except the input of radioactive isotope at the recharge zone. If the aquifer is recharged by multiple sources of fresh water [*Plummer et al.,* 1998], along the groundwater flow path, new sources of radioactive isotopes will be added into the system. In order keep the mathematical formulation simple enough to show the effect of diffusion along the aquifer-aquitard contact on groundwater dating, we will not consider the case of mixing of several fresh water sources. Under all these assumptions, the governing equations [Bear, 1972, Freeze and Cherry, 1979] and initial and boundary conditions for transport of radioactive isotopes in both the aquifer and aquitard of this case are as follows. For the aquifer,

$$R\frac{\partial C}{\partial t} = D_x\frac{\partial^2 C}{\partial x^2} + D_z\frac{\partial^2 C}{\partial z^2} - v\frac{\partial C}{\partial x} - \lambda RC\,, \qquad (4\text{-}1)$$

$$C(x=0,z,t)=C_0, \tag{4-2}$$

$$C(x=+\infty,z,t)=0, \tag{4-3}$$

$$\frac{\partial C(x,z=0,t)}{\partial z}=0, \tag{4-4}$$

$C(x,z,t=0)=0$, for $x>0$, (4-5)

and for the aquitard,

$$R_1\frac{\partial C_1}{\partial t}=D_{01}\frac{\partial^2 C_1}{\partial z^2}-\lambda R_1 C_1, \tag{4-6}$$

$$C_1(x,z=B,t)=C(x,z=B,t), \tag{4-7}$$

$$\theta_1 D_{01}\frac{\partial C_1(x,z=B,t)}{\partial z}=\theta D_z\frac{\partial C(x,z=B,t)}{\partial z}, \tag{4-8}$$

$$C_1(x,z=+\infty,t)=0, \tag{4-9}$$

$$C_1(x,z,t=0)=0, \tag{4-10}$$

where C and C_1 represent the residential concentrations in the aquifer and aquitard, respectively; δt is the dirac delta function. The input function C_0 states that the radioactive tracer was released to the groundwater in the aquifer at constant concentration C_0 at the left boundary of the domain (x=0) from t = 0; v is the average pore velocity of groundwater flow in the aquifer; D_x and D_z are the longitudinal and vertical hydrodynamic dispersion coefficients respectively for the aquifer, and $D_x=\alpha_x v+D_0$, $D_z=\alpha_z v+D_0$, where α_x and α_z are the longitudinal and vertical dispersivities, respectively, D_0 is the molecular diffusion coefficient of the solute in pure water [*Bear*, 1972]. D_{01} is the effective molecular diffusion coefficient in the aquitard; B is the half thickness of the aquifer; θ_1 and θ are the porosities of the aquitard and aquifer, respectively; and t is time. λ is the decay constant of radioactive isotopes. The effective

molecular diffusion in the aquitard is $D_{01} = \tau_1 D_0$, where τ_1 is tortuosity. Taking into account that the radioactive nuclides can generally be more effectively retarded in the aquitard than the aquifer because of the presents of clay minerals in the aquitard, different retardation factors R and R_1 are used here for aquifer and aquitard, respectively. Retardation of solute particles is caused by sorption and desorption process at mineral surface. It can be described by $R = 1 + \frac{1-\theta}{\theta} K_d$, where K_d is the distribution coefficient between the groundwater and mineral.

Eqs. (4-1) is the advection-dispersion equation of solute transport in the aquifer with retardation, first-order radioactive decay (*Bear,* 1972, p618). Biodegradation of environmental tracer such as CFCs can be treated in the same way. *Cook et al.* [1995] reported the half-life of CFC-11 was 0.9-1.7 year and that of CFC-12 is > 90 years. From the half-life values, once can calculate the decay constant by the equation $\lambda = \ln 2 / T_{1/2}$, where $T_{1/2}$ is the half life of the radioactive isotopes. Eqs. (4-2) is the input function of the radioactive nuclides. We use a constant concentration input function here for simplicity, but it can be easily changed to an arbitrary function of time. Eqs. (4-3) is the boundary conditions at the right end of the aquifer. Eqs. (4-4) is the no mass flux condition at z=0 because of the geometric symmetry about z=0. Eqs. (4-5) is the initial condition in the aquifer. In some groundwater dating methods, for instance, $^{36}Cl/Cl$ method, the initial input concentration of radioactive isotopes is not that easy to find. But in order to apply such a method in hydraulic study, one has to find a way to quantify the initial value. A common approach is to use the sum of the concentrations of radioactive

and radiogenic isotopes as the initial concentration of radioactive isotopes. It is important to point out that this approach implies that the concentration of radiogenic isotopes should be zero or small enough to be safely neglected. Another approach is to use multiple isotopes to date groundwater. *Lehmann et al*. [2003] was able to determine the initial value of ^{36}Cl by calibrating the ^{36}Cl /Cl data by ^{81}Kr/Kr data. In-situ release of radiogenic isotopes from the rock matrix, both aquifer and aquitard, to the groundwater can be important process. In their study of radiogenic ^{4}He of the Sturgeon Falls Site, Canada, *Solomon et al.* [1996] reported ^{4}He release rate at 130 $ucm^3m^{-3}yr^{-1}$, which is about 300 times greater than can be supported by the in-situ decay of U-Th series nuclides. They believed the source of the excessive radiogenic ^{4}He came from the unconsolidated aquifer solids whose protolith is the metamorphic rocks of the Canadian Shield (Age > 1Ga) that contain large quantities of ^{4}He. In this paper, we will focus on the effect of diffusion along the aquifer-aquitard boundary and the consequence and implication on groundwater dating, so mixing of different groundwater sources and in-situ production of radiogenic isotopes will not be addressed. Eqs. (4-6) is the diffusion equation in the aquitard, Eqs. (4-7) and (4-8) are the continuity of concentration and mass flux at the upper aquitard-aquifer boundary at $z=B$, respectively, Eqs. (4-9) is the vertical boundary condition for a sufficiently thick aquitard, and Eqs. (4-10) is the initial condition in the aquitard.

It is not easy to formulate a group of equations for the transport of radiogenic isotopes because the concentration of radiogenic isotopes depending on that of the radioactive isotopes. The radiogenic isotope will accumulate with time from radioactive

decay, and the accumulation rate equals decay rate of radioactive isotope. So we cannot know the concentration of radiogenic isotopes until we solve the concentration of radioactive isotopes. Based on the complexity of the solutions of radioactive isotopes, it seems finding concentration of radiogenic isotopes in this problem via analytical approach is very difficult, if not impossible, so all the discussions in this paper will focus on radioactive isotopes only.

We define dimensionless terms as follow:

$$x_D = \frac{x}{B}\sqrt{\frac{D_z}{D_x}}\ ,\ z_D = \frac{z}{B}\ ,\ t_D = \frac{D_z}{RB^2}t\ ,\ C_D = \frac{C}{C_0}\ ,\ C_{1D} = \frac{C_1}{C_0}\ ,\ \gamma = \frac{vB}{\sqrt{D_x D_z}}\ ,\ \beta_1 = \frac{D_{01}}{D_z}\ ,$$
$$\sigma_1 = \frac{\theta_1}{\theta}\ ,\ \varepsilon_1 = \frac{R}{R_1}\ ,\kappa = \frac{B^2 R\lambda}{D_z}\ , \qquad (4\text{-}11)$$

where subscript "*D*" represents the dimensionless term, γ is the Peclet number [*Bear*, 1972]. Definitions of all the dimensionless terms used in this chapter can be found in Table 4-2. After transforming above Eqs. (4-1) - (4-10) into dimensionless forms, apply the Laplace transform to the governing equations and boundary conditions will result in the following equation group. For the brevity of presentation, all the discussions in the rest of this paper are in dimensionless forms and the subscript "*D*" is removed.

$$p\overline{C} = \frac{\partial^2 \overline{C}}{\partial x^2} + \frac{\partial^2 \overline{C}}{\partial z^2} - \gamma\frac{\partial \overline{C}}{\partial x} - \kappa\overline{C}\ , \qquad (4\text{-}12)$$

$$\overline{C}(x=0, z, p) = 1\ , \qquad (4\text{-}13)$$

$$\overline{C}(x=+\infty, z, p) = 0\ , \qquad (4\text{-}14)$$

$$\frac{\partial \overline{C}(x, z=0, p)}{\partial z} = 0\ , \qquad (4\text{-}15)$$

$$p\overline{C}_1 = \varepsilon_1\beta_1\frac{\partial^2 \overline{C}_1}{\partial z^2} - \kappa\overline{C}_1\ , \qquad (4\text{-}16)$$

$$\overline{C}_1(x, z=1, p) = \overline{C}(x, z=1, p), \tag{4-17}$$

$$\beta_1\sigma_1 \frac{\partial \overline{C}_1(x, z=1, p)}{\partial z} = \frac{\partial \overline{C}(x, z=1, p)}{\partial z}, \tag{4-18}$$

$$\overline{C}_1(x, z=+\infty, p) = 0, \tag{4-19}$$

where $\overline{C}$ and $\overline{C}_1$ are the Laplace transforms of C and C_1, respectively, and p is the Laplace transform parameter in respective to the dimensionless time.

The procedure of solving the above equation group of (4-12)-(4-19) is given in APPENDIX C. The derived solutions for $\overline{C}$ and $\overline{C}_1$ are:

$$\overline{C} = \sum_{n=0}^{\infty} \frac{4\sin\omega_n}{p(\sin(2\omega_n)+2\omega_n)} \exp\left[\left(\frac{\gamma - \sqrt{\gamma^2 + 4(p+\kappa+\omega_n^2)}}{2}\right)x\right]\cos(\omega_n z), \tag{4-20}$$

$$\overline{C} = \sum_{n=0}^{\infty} \frac{2\sin(2\omega_n)}{p(\sin(2\omega_n)+2\omega_n)} \exp\left[\left(\frac{\gamma - \sqrt{\gamma^2 + 4(p+\kappa+\omega_n^2)}}{2}\right)x + (1-z)\sqrt{\frac{p+\kappa}{\varepsilon_1\beta_1}}\right], \tag{4-21}$$

where the frequency ω_n is determined via (C-6) and $F(\omega_n)$ is given in Eqs. (C-8) of APPENDIX C.

In geologically reality, the input function of radioactive isotopes is changing with time. Tritium concentration in the atmosphere is very small before the above-ground testing of thermo-nuclear weapons around 1950s'. Its concentration reaches a peak value and then continuously drops down after the test stop treaty in 1963. A general input function (*f(t)*)can be adopted in the formulation instead of pulse injection to deal with more complex input scenarios. For example, if an aquifer is continuously recharged by river water during the past 50 years, the tritium (^{3}H) input functions *f(t)* can be

calculated from the atmospheric tritium concentration of the past 50 years (Figure 7.6 and 7.7 of *Kendall & McDonnell* [1998]). If an general input function *f(t)* is used, Eqs. (4-2) will be replaced by

$$C(x=0,z,t)=f(t), \tag{4-22}$$

and Eqs. (4-13) will be replaced by

$$\overline{C}(x=0,z,p)=F(p). \tag{4-23}$$

Where *F(p)* is the Laplace transformation of *f(t)*. Following the same procedure described in APPENDIX C, one can obtain the following corresponding solutions for $\overline{C}$ and $\overline{C_1}$ which are differ from Eqs. (4-20) and (4-21) only by input function: replacing the Laplace transformation of the dirac delta function (which is simply 1) by the Laplace transformation of *f(t)* (which is *F(p)*):

$$\overline{C}=\sum_{n=0}^{\infty}\frac{4F(p)\sin\omega_n}{\sin(2\omega_n)+2\omega_n}\exp\left[\left(\frac{\gamma-\sqrt{\gamma^2+4(p+\kappa+\omega_n^2)}}{2}\right)x\right]\cos(\omega_n z), \tag{4-24}$$

$$\overline{C}=\sum_{n=0}^{\infty}\frac{2F(p)\sin(2\omega_n)}{\sin(2\omega_n)+2\omega_n}\exp\left[\left(\frac{\gamma-\sqrt{\gamma^2+4(p+\kappa+\omega_n^2)}}{2}\right)x+(1-z)\sqrt{\frac{p+\kappa}{\varepsilon_1\beta_1}}\right], \tag{4-25}$$

4.2.3. Solute transport in an aquifer bounded by an upper aquitard and lower bedrock

If the aquifer is bounded by an upper aquitard and lower bedrock which is treated as a no-flux boundary for transport (Figure 4-1B), the concentrations in the aquifer and aquitard can be easily obtained by modifying the solutions derived in section 4.2.2. Eqs (4-4) basically described a no vertical transport along the straight line x = 0, which is the true case because this line is the mirror symmetry line of the aquifer-aquitard system in

section 4.2.2. In case of an aquifer bounded by bedrock, the bedrock is generally treated as a no-flow boundary by hydro-geologists. We set the origin of our coordinate system at the contact between aquifer and bedrock and x axis is along the contact. The thickness of the aquifer is still 2B, the same as in Figure 4-1A. If redefining the dimensionless terms of Eqs. (3-11) by replacing B with $2B$, then the two problems become mathematically identical, all the solutions derived in section 4.2.2 can be directly applied to the case of this section.

4.2.4. Solute transport in an aquifer bounded by different upper and lower aquitards

The upper and lower aquitards were deposited at different geologic time, so generally speaking, this two aquitards will not process the identical hydraulic properties, because they may composed by different geologic materials in different texture and structure. For instance, *Ball et al.* [1997a] has reported an upper aquitard of orange silty clay loam and a lower aquitard of dark gray silt loam adjacent to the aquifer at Dover Air Force Base. It is interesting to know whether the differences in the upper and lower aquitards have some impact on the transport of radioactive isotopes. The river water with relatively younger age is leaking into the Upper Floridan aquifer through a shallow semi-confined aquifer (*Plummer et al.* [1998]), additional radioactive isotopes (^{3}H) is added in to groundwater during this process; while the lower aquitard can be the sources of radiogenic isotopes (^{4}He) diffusing into the main aquifer. We will derive radioactive isotope transport in an aquifer bounded by different upper and lower aquitards in this

section: they have different retardation factor, porosity, tortuosity, and so different diffusion coefficient. Because of these differences, the concentrations in the upper and lower aquitards are generally different, and are denoted as C_1 and C_2, respectively.

Using the coordinate system of Figure 4-1C, unless otherwise pointed out, we use subscript 1 for the upper aquitard and 2 for the lower aquitard, so R_1, R_2, θ_1, θ_2, D_{01} and D_{02} are the retardation factor, porosity and effective diffusion coefficient of upper and lower aquitard , respectively. This rule also obeyed in naming those dummy parameters used during derivation. We set the origin of our coordinate on top of the lower aquitard, x axis running along the contact between the lower aquitard and the aquifer, and y axis points up. Replacing *B* in Eqs. (4-11) by 2B results the following new dimensionless parameters:

$$\beta_2 = \frac{D_{02}}{D_z},\ \sigma_2 = \frac{\theta_2}{\theta}, C_{2D} = \frac{C_2}{C_0}, \varepsilon_2 = \frac{R}{R_2}, \tag{4-26}$$

We can describe the lower aquitard using the following equations:

$$R_2 \frac{\partial C_2}{\partial t} = D_{02} \frac{\partial^2 C_2}{\partial z^2} - \lambda R_2 C_2 \tag{4-27}$$

$$C_2(x, z = 0, t) = C(x, z = 0, t) \tag{4-28}$$

$$\theta_2 D_{02} \frac{\partial C_2(x, z = 0, t)}{\partial z} = \theta D_z \frac{\partial C(x, z = 0, t)}{\partial z} \tag{4-29}$$

$$C_2(x, z = +\infty, t) = 0 \tag{4-30}$$

$$C_2(x, z, t = 0) = 0 \tag{4-31}$$

Equations (4-27) – (4-31) are analogue to Eqs. (4-6)-(4-10). After changing Eqs. (4-27)-(4-31) into dimensionless form, using the dimensionless terms defined in Eqs. (4-11) and

(4-26), and performing Laplace transform on the resulted equations, one can reach the following equations:

$$\frac{\partial^2 \bar{C}_2}{\partial z^2} - \frac{\kappa + p}{\varepsilon_2 \beta_2} \bar{C}_2 = 0 \tag{4-32}$$

$$\bar{C}_2(x, z = 0, p) = \bar{C}(x, z = 0, p) \tag{4-33}$$

$$\beta_2 \sigma_2 \frac{\partial \bar{C}_2(x, z = 0, p)}{\partial z} = \frac{\partial \bar{C}(x, z = 0, p)}{\partial z} \tag{4-34}$$

$$\bar{C}_2(x, z = +\infty, p) = 0 \tag{4-35}$$

Adding Eqs. (4-32) - (4-35) to Eqs. (4-12) - (4-19), one will be able to derive the concentrations in the aquifer and in the upper and lower aquitards. The details of mathematical modeling are shown in APPENDIX D.

For the input function of constant concentration at x=0, the solutions are

$$\bar{C} = \sum_{n=0}^{\infty} A_n \exp\left[\left(\frac{\gamma - \sqrt{\gamma^2 + 4(p + \kappa + \omega_n^2)}}{2} \right) x \right] \cos(\omega_n z + \mu_n), \quad 0 \le z \le 1, \tag{4-36}$$

$$\bar{C}_1 = \sum_{n=0}^{\infty} A_n \exp\left[\left(\frac{\gamma - \sqrt{\gamma^2 + 4(p + \kappa + \omega_n^2)}}{2} \right) x \right] \cos(\omega_n + \mu_n) \exp\left[\sqrt{\frac{\kappa + p}{\varepsilon_1 \beta_1}} (1 - z) \right], \; 1 \le z \le \infty . \tag{4-37}$$

$$\bar{C}_2 = \sum_{n=0}^{\infty} A_n \exp\left[\left(\frac{\gamma - \sqrt{\gamma^2 + 4(p + \kappa + \omega_n^2)}}{2} \right) x \right] \cos(\mu_n) \exp\left[\sqrt{\frac{\kappa + p}{\varepsilon_2 \beta_2}} z \right], \; -\infty \le z \le 0, \tag{4-38}$$

where

$$A_n = \frac{4F_1(\omega_n, \mu_n)}{pF_2(\omega_n, \mu_n)}, \tag{4-39}$$

and $F_1(\omega_n, \mu_n)$ and $F_2(\omega_n, \mu_n)$ are given in (D-11). If the general input function *f(t)* is used, then replace Eqs. (4-13) by (4-23), and the final solutions are identical to Eqs. (4-36) to (4-38) except that A_n is replaced by

$$A_n = \frac{4F(p)F_1(\omega_n, \mu_n)}{F_2(\omega_n, \mu_n)}, \tag{4-40}$$

4.3. Results Analysis

The solutions in Laplace domain derived in previous sections can be numerically inversed to get concentration at real time domain using the multiple precision Stehfest algorithm. The following discussion is based on the numerical inversion of Laplace domain solutions. *Kendall & McDonnell* (1998) summarized effects of different transport processes on the groundwater age dating. Here we try to manifest some of those effects from our solutions of radioactive tracer transport in aquifer bounded by identical aquitards, developed in Section 4.2.2 because the solutions are relatively simpler than the case of an aquifer bounded by different aquitard.

4.3.1 Default values of parameters

The default parameters for the following discussion are included in Table 1. As examples, the first-type boundary condition (constant concentration) is used in all the following discussion. The default radioactive tracer is tritium (^{3}H), so the default value of half-life is 12.3 yr and the decay constant is calculated as $\lambda = \frac{\ln 2}{T_{1/2}} = \frac{\ln 2}{12.3 yr * 31536000 s / yr} = 1.786 * 10^{-9} s^{-1}$. The self diffusion coefficient of ^{3}H

in dilute water $1.57*10^{-9}$ m^2/s [*Wang et al.*, 1952] is chosen to be the default molecular diffusion coefficient D_0 for aquitard. The tortuosity of aquitard is set to 0.75, so the effective diffusion coefficient $D_{01}=\tau D_0=1.18*10^{-9}$ m^2/s. The average pore velocity v is chosen to be 0.10m/day or1.16×10^{-6} m/s. The same values of D_0 and v were also used in *Sudicky et al.* [1985]. For a field- scale dispersion problem, we choose the longitudinal dispersivity a_x=1m. The transverse dispersivity is expected to be 1/10 of the longitudinal one as a_z=0.1m. Such a choice is consistent with field-scale dispersion [*Domenico and Schwartz*, 1998; *Fetter*, 1999] but is much greater than the local dispersivity used in the laboratory experiment of *Sudicky et al.* [1985], which is 0.001m. Therefore, the corresponding dispersion coefficients are $D_x = a_x v = 1.16\times10^{-6}$ m^2/s, and $D_z = a_z v = 1.16\times10^{-7}$ m^2/s if neglecting the molecular diffusion. The aquifer thickness is 2*B*=20 m. The corresponding Peclet number γ is 31.6. A default porosity value is set to 0.36 for both aquifer and aquitard. The same porosity is used for the aquitard in *Sudicky et al.* [1985]. *Bethke and Johnson* [2002] concluded that the effect of mixing of older groundwater from the aquitard to aquifer does not depend on the mixing rate, but solely depend on the ratio of fluid volume of the aquitard to the aquifer based on their analysis of age mass transport under steady state condition. The default values of parameters used in this chapter are summarized in Table 4-1.

4.3.2. Effect of Radioactive decay

Figures 4-2A, 4-2B and 4-2C show the effects of radioactive decay. We use two typical isotopes, ^{3}H and ^{14}C, as examples. The half-life of ^{3}H is about 12.3 years, so it is good to date very young groundwater (younger than 50 years from present), while ^{14}C has a half-life of 6370, which make it good for dating relatively older groundwater, on the magnitude of 10,000 years. A constant concentration input function is used and the results shown in figures 4-2A through 4-2C are break through curve at the x axis or the line of z = 0. Z=0 is the line where the diffusion along the aquifer-aquitard boundary has least effect, so it is good to be used to investigate the effects of other parameters. Because of the radio active decay, the concentration is usually much less than unit 1. Dimensionless concentration 1 is supposed to be the steady state concentration without radioactive decay (Figure 4-2A). We also noticed on Figure 4-2A that the maximum concentration at short distance (x = 5) is much higher than that at longer distance (x = 10). This is not unexpected because of the radioactive decay. Radioactive decay causes there are fewer particles to be transported so will tend to decrease the concentration. Figure 4-2B shows the comparison among break through curves of the cases of no radioactive decay, ^{3}H and ^{14}C at dimensionless distance x = 10. We observed that the concentrations of ^{3}H are clearly smaller than that of no decay case, while ^{14}C concentration shows unobservable differences with no decay. It can be easily understand if one can change our dimensionless term into dimension term. Using the default value we listed in Table 1, dimensionless time 1 is roughly 100 years, which is about 8 times of the half-life of ^{3}H, but is only 1/60 of ^{14}C's half-life, so ^{14}C show little differences

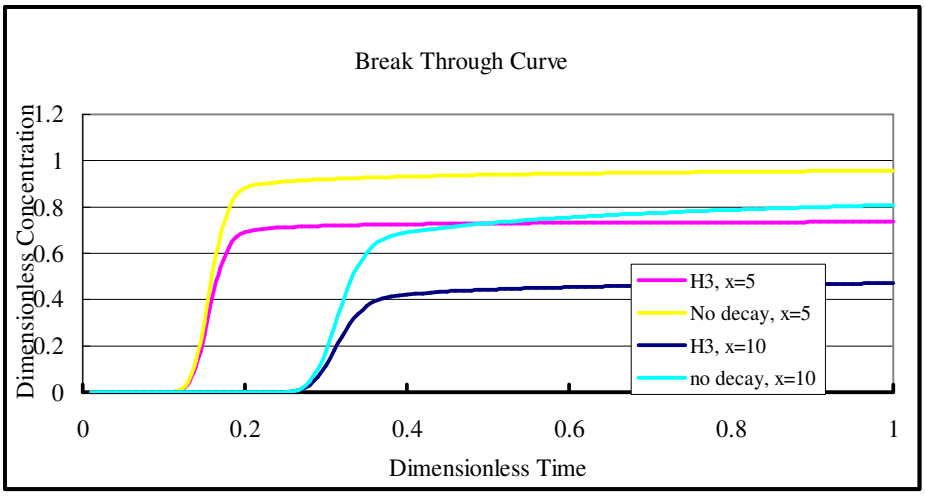

Figure 4-2A. Break through curve at x=5 and 10 for radioactive tracer (^{3}H) and non-radioactive tracer, shown the result of radioactive decay.

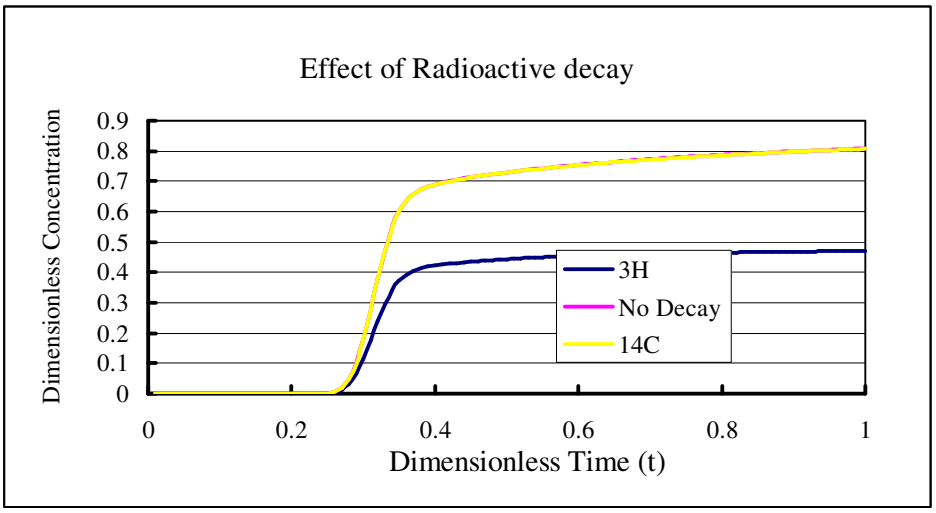

Figure 4-2B. Break through curve for ^{3}H, ^{14}C and non-radioactive tracer at x = 10.

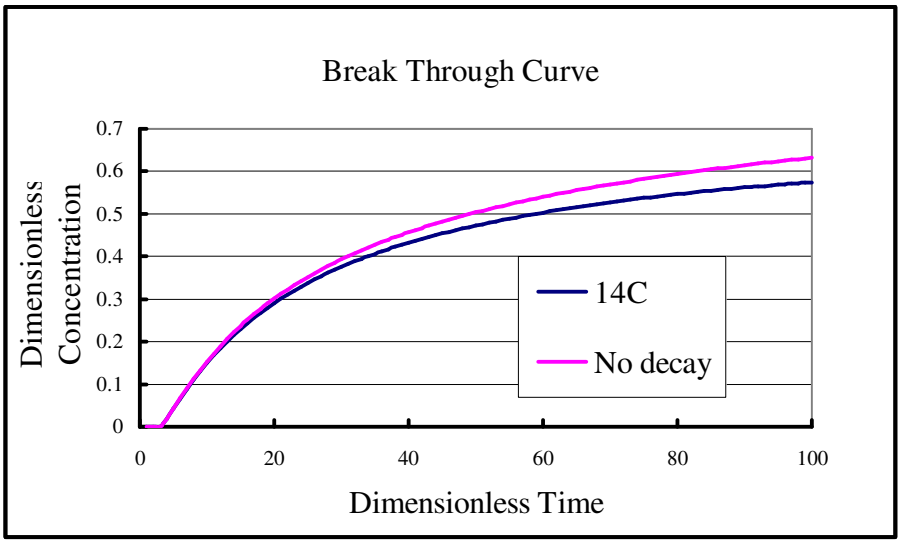

Figure 4-2C. Break through curve of ^{14}C and non-radioactive tracer at x=100.

compared with no decay. If we extended our observation to 100 dimensionless time, then the effect of radioactive decay of ^{14}C appears (Figure 4-2C).

4.3.3. Effect of retardation

Retardation will cause the solute transport slow down, as if the pore velocity is decreased. From piston flow model, it is easy to understand if the radioactive tracers are retarded, then the groundwater age from data collected from such an aquifer will be older than actual age, or the actual pore velocity will be underestimated by the same factor as the retardation factor. The retardation factor of the aquifer will not be significantly larger than 1, because the aquifer are mainly composed by sand sized

particles. Unless the sand particles are covered by organic deposition, the retardation effect usually can be safely neglected. Here we change the retardation factor of aquitard to manifest the effect of retardation on radioactive tracer transport. The retardation factor can be varied in quite big range, based on different aquitard materials. *Liu and Ball* [1999], in their analytical study of diffusive contaminant transport in two aquitard layers (orange silty clay layer OSCL and dark gray silty layer DGSL), used retardation factors of 2 and 45 for PCE in OSCL and DGSL, 1.4 and 20 for TCE in OSCL and DGSL, respectively. We use the aquitard retardation factor of 1, 5 and 10 to show the retardation effect on radioactive tracer transport. Figure 4-3 shows the break through curves along the x axis for the 3 different R_1s at x = 10. Even for the $R_1 = 1$ case (no retardation at the aquitard), the maximum concentration is only around 0.5 -0.6, instead of 1, which is because of the radioactive decay. We set our default value of decay constant as that of ^3H. Readers will notice that if compare Figure 4-3 with Figure 4-2A. When the retardation factor increase, the maximum concentration of the break though curve decrease, as we expected.

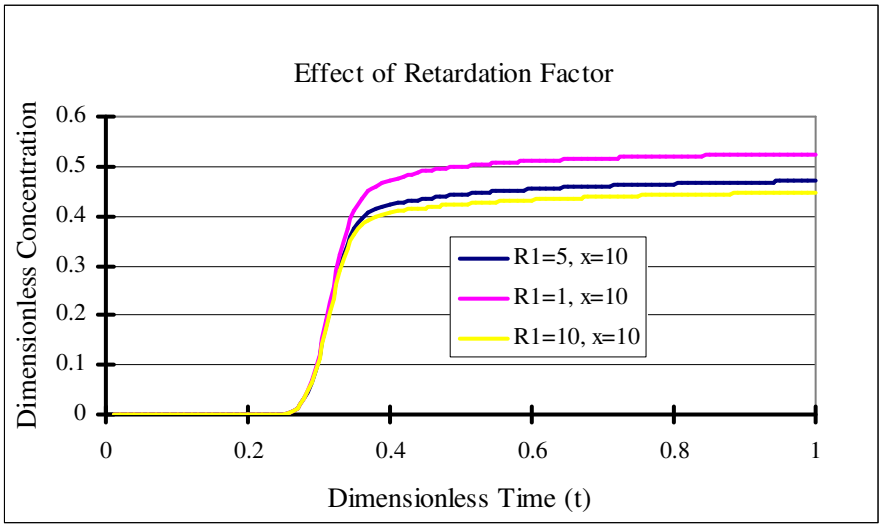

Figure 4-3. Break through curves show the effects of retardation.

4.3.4. Horizontal concentration distribution

The horizontal concentration distribution in the aquifer can be calculated form Eqs. (4-20). Figures 4-4A and B shows the horizontal concentration curve of ^{3}H. It is worthwhile to note that the concentration of ^{3}H are nearly at steady state after short time (both t = 0.5 and t = 1 at Figure 4-4A), which can be proved by comparing the steady state concentration curve along x axis with the results of Eqs. (4-20). A steady state solution can be derived from Eqs. (4-20) as:

$$C = \sum_{n=0}^{\infty} \frac{4\sin\omega_n}{(\sin(2\omega_n)+2\omega_n)} \exp\left[\left(\frac{\gamma-\sqrt{\gamma^2+4(\kappa+\omega_n^2)}}{2}\right)x\right]\cos(\omega_n z)\,. \qquad (4\text{-}41)$$

Where C is the concentration in real time domain. Derivation of Eqs. 4-41 is based on the relationship:

$$f(t)\big|_{t\to\infty} = pF(p)\big|_{p\to 0} \qquad (4\text{-}42)$$

Using the same relationship, we can derive the steady state solution for the aquitard as:

$$C = \sum_{n=0}^{\infty} \frac{2\sin(2\omega_n)}{(\sin(2\omega_n)+2\omega_n)} \exp\left[\left(\frac{\gamma - \sqrt{\gamma^2 + 4(\kappa+\omega_n^2)}}{2}\right)x + (1-z)\sqrt{\frac{\kappa}{\varepsilon_1\beta_1}}\right], \qquad (4\text{-}43)$$

where ω_n in Eqs. (4-41) and (4-43) are the solution of Eqs. (C-6) with *p=0.* When time t increase from 0.5 to 1, the solute front moved forward, but the part between x = [0, 4] seems to have very little change. It is interesting to see that this part can be fit by a straight line shown on Figure 4-4B perfectly, with R = 0.9998. Results of steady state solution at this part follow almost the same straight line, with unnoticeable slope different. (Figures 4-4B and 4-4C). We haven't figure out why solute concentration follow a straight line yet, but once this is proved to be true, or in other words, the early part of the transport path reaches steady state in relatively short time, then a big problem is post on groundwater age dating using radiometric techniques: if ratio of the radioactive isotope does change with time, how can we find an meaningful age data from these areas?

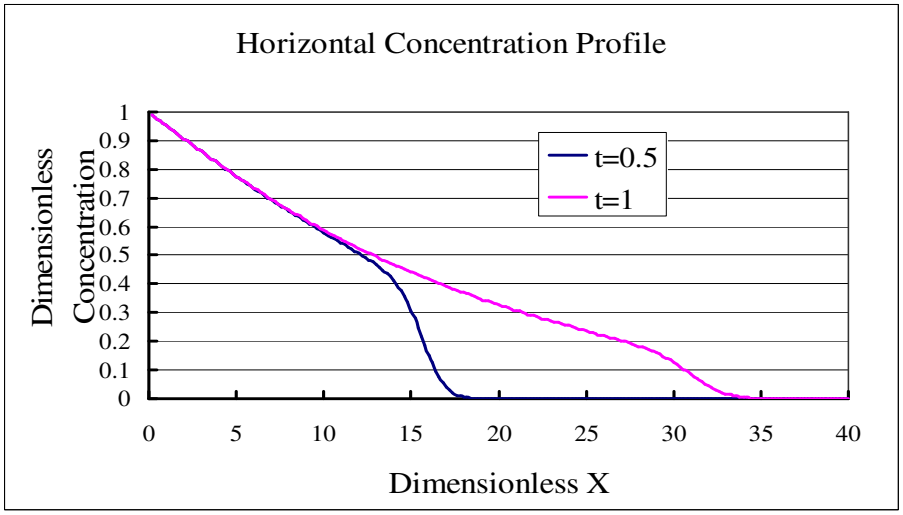

Figure 4-4A. Horizontal concentration profile of ^3H at t =0.5 and 1.

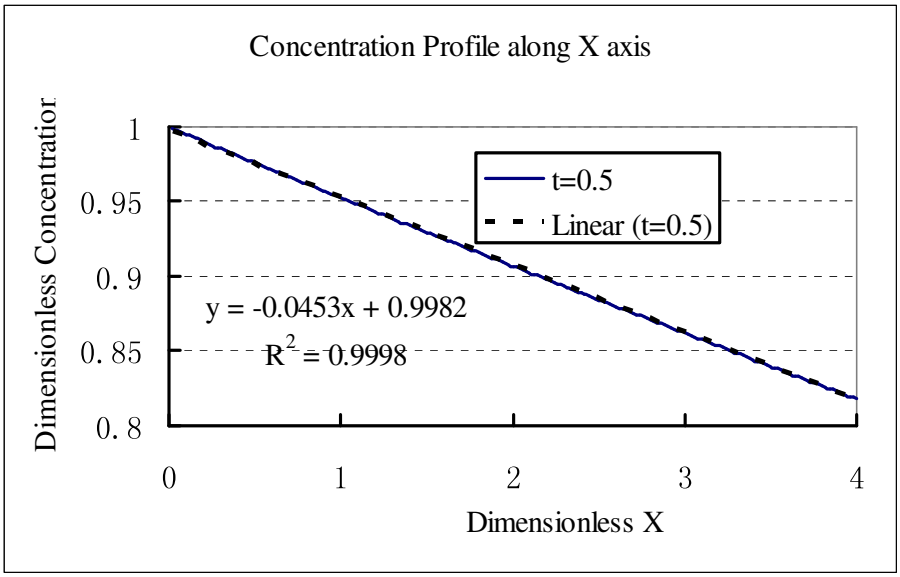

Figure 4-4B. Concentration distribution along X axis with a perfect trend line.

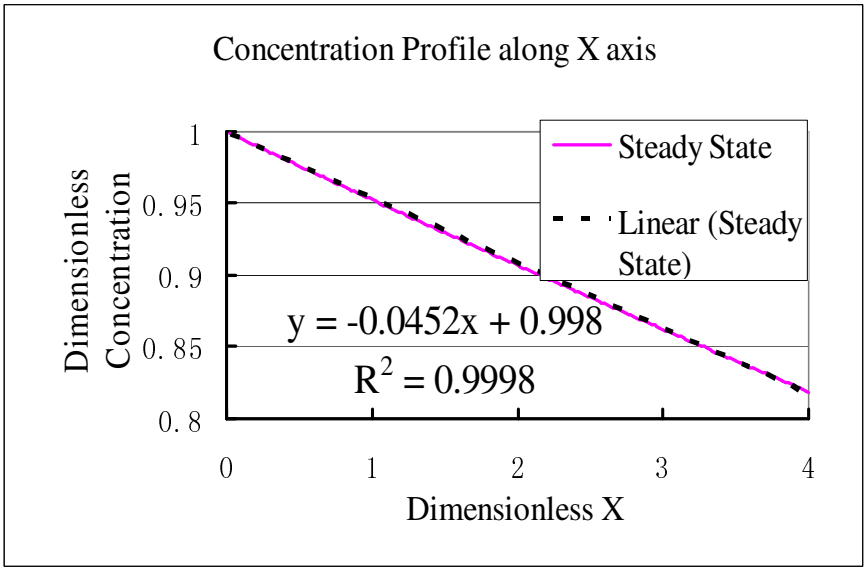

Figure 4-4C. Horizontal concentration distribution at steady state with a trend line.

4.3.5. Vertical concentration profile across the aquifer-aquitard boundary

The effects of aquitard on solute transport in aquifer-aquitard system are mainly expressed as diffusion. To investigate the effect of diffusion, we constructed several vertical concentration profiles based on Eqs. (4-20). A sample plot is shown as Figures 4-5A and 4-5B. Figure 4-5A is at short distance and short time, while Figure 4-5B is at relatively longer distance and later time. Both plots clearly shows that there is fairly large portion of the solute is transporting in the aquitard, so we cannot simply treat the aquitard as an impermeable boundary.

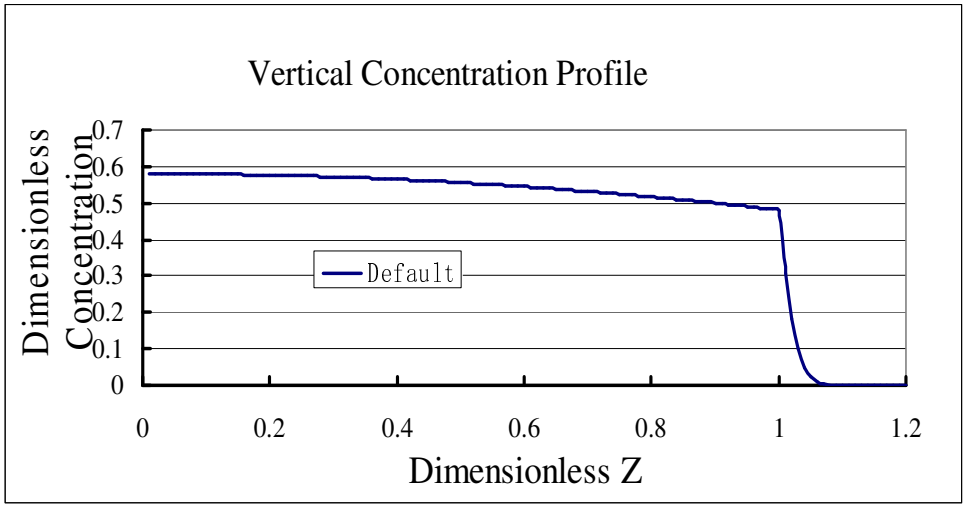

Figure 4-5A. Vertical concentration profile across the aquifer aquitard boundary at t=0.5 and x=10.

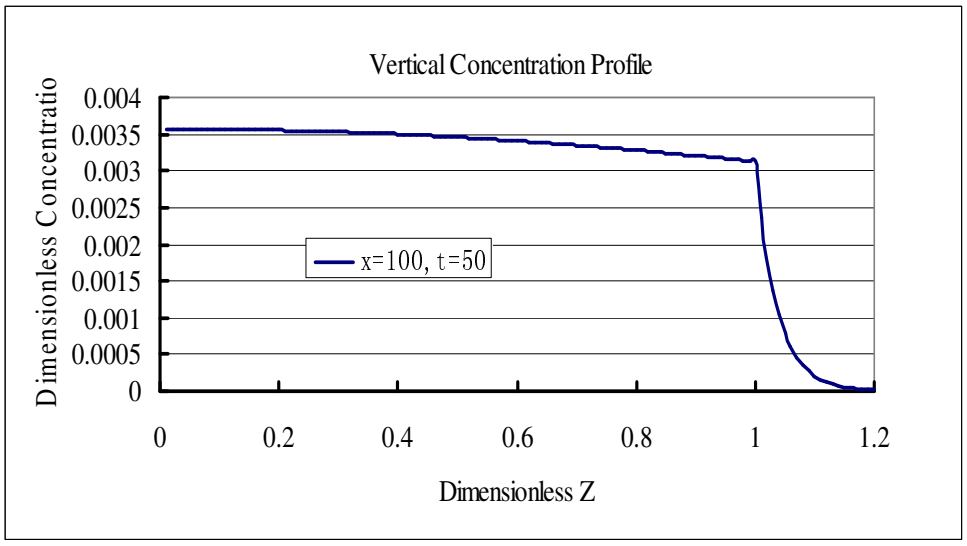

Figure 4-5B. Vertical concentration profile across the aquifer-aquitard boundary at x =100, t = 50.

4.3.6. Mass diffused into the aquitard

We notice the diffusion from the aquifer to the aquitard is an important process by looking at Figure 4-5 A and B. It is interesting to know how much mass was stored in the aquitard due to aquitard diffusion. The total mass per unit thickness along the *y*-axis (perpendicular to the *xz* plane) in the aquitard in Laplace domain, $\overline{M}_1$, can be obtained through the following integration:

$$\overline{M}_1 = \int_0^\infty dx \int_1^\infty \overline{C}_1 dz \,. \qquad (4\text{-}44)$$

This can be done straightforwardly. For instance, using Eqs. (4-25) as an example, one has

$$\overline{M}_1 = \sum_{n=0}^{\infty} \frac{2F(p)\sin(2\omega_n)}{\sin(2\omega_n)+2\omega_n} \times \left[\frac{\sqrt{\gamma^2 + 4(p+\kappa+\omega_n^2)} - \gamma}{2} \times \sqrt{\frac{p+\kappa}{\varepsilon_1 \beta_1}} \right]^{-1} . \qquad (4\text{-}45)$$

Inverse Laplace transform of $\overline{M}_1$ will result in the solution in real time domain M_1. *Zhan et al.* [2006] compared the mass diffused into the aquitard from the aquifer calculated from so called "new method" and "old method". The two methods differ in the way they treat the diffusion along the aquifer-aquitard boundary. The old method treats the diffusion flux as a volume averaged source term which is added to the governing equation of the main aquifer. The new method proposed by *Zhan et al.* [2006], on the other hand, treated the aquifer and aquitard contact as a continuity boundary of both solute concentration and vertical flux. The old method ended up with a one dimensional governing equation in aquifer, while the new method will have to solve a 2-dimensional equation, but *Zhan et al.* [2006] proved that the old method will tend to over estimate the diffusion loss from the aquifer to the aquitard, as a consequence, the concentration of the solute in the aquifer will be underestimated. The new method is more physically sound and should be able to give more accurate results. Figures 4-6A and 4-6B show the accumulated mass diffused from the aquifer into the aquitard for different vertical dispersivity and different effective diffusion coefficient. Several observations can be made from these two Figures. First, the total diffusive mass depends on the value of α_z. A greater α_z will result in greater amounts of mass diffused to the aquitard. A greater α_z implies the vertical movements of solute particles are more active, thus more particles will be available for diffusion. The effective diffusion coefficient

controls mass diffusion process, which seems intuitive. The second observation is that greater the effective diffusion coefficient, larger will be the total mass diffused into the aquifer. One can understand fast diffusion process will be able to catch more particles along the aquifer-aquitard boundary, thus it will be able to transport more particles from the aquifer to the aquitard.

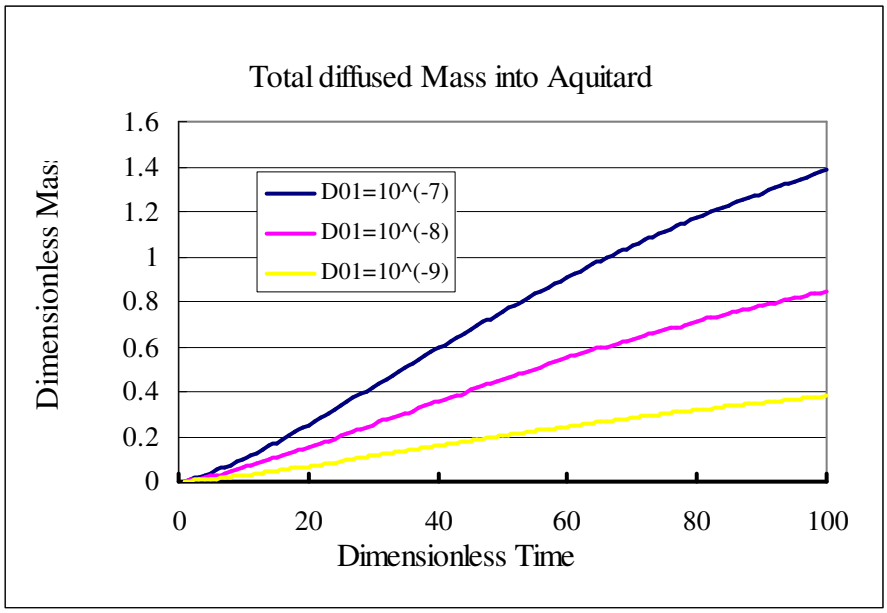

Figure 4-6A. Total mass diffused into aquitard at $\alpha_z = 0.1$m.

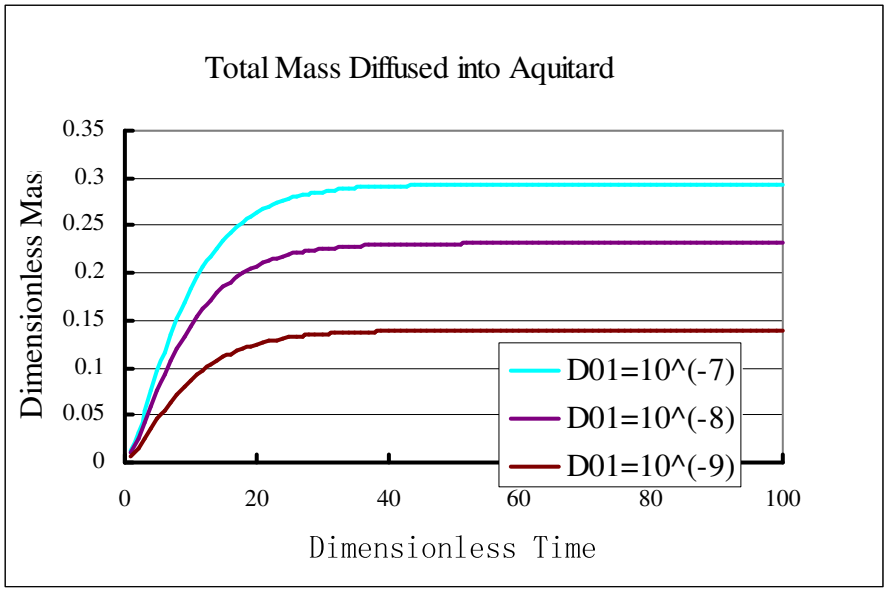

Figure 4-6B. Total mass diffused into aquitard at $\alpha_z = 0.01$m.

The last observation we can made is that on Figure 4-6B, the total mass diffused into the aquitard reaches steady state at dimensionless time around 60. Steady state means the mass diffused into the aquitard are balanced by the radioactive decay. Also steady state total mass of radioactive isotopes means the age distribution in the aquitard reach steady state. This observation agreed with *Bethke and Johnson* [2002], they predicted that the age distribution in the aquitard will reach a steady state condition after some relaxation time. This relaxation time can be found out by the formula $t_r = B^2/D_0$ [revised after *Carslaw and Jaeger,* 1959]. In our case, we use default value of B = 10m, $D_0 = 1.57*10^{-9}$ m^2/s, and result in a relaxation time t_r = 2620 year, which equals our

dimensionless time t_D = *73*. The total mass diffused into the aquitard can be calculated from Eqs. 4-45. Recall the relationship 4-42, applying it on Eqs. (4-45) results:

$$M_1\big|_{t\to\infty} = (p\bar{M}_1)\big|_{p\to 0} = \sum_{n=0}^{\infty} \frac{\sin(2\omega_n)}{\sin(2\omega_n)+2\omega_n} \times \left[\frac{\sqrt{\gamma^2 + 4(\kappa+\omega_n^2)} - \gamma}{2} \times \sqrt{\frac{\kappa}{\varepsilon_1\beta_1}} \right]^{-1} \quad .(4\text{-}46)$$

Where the parameter ω_n are the roots of the following equation:

$$\omega_n \tan\omega_n = \sigma_1 \sqrt{\frac{\beta_1\kappa}{\varepsilon_1}} \, . \qquad (4\text{-}47)$$

where ω_n are a series of constant roots, depending on neither *p* nor *t.* Eqs. 4-45 and 4-46 then can be used to calculate the steady state total radioactive mass diffused from the aquitard to the aquifer.

4.4. Apply the Results to Groundwater Dating

Any groundwater dating techniques require a closed system for the testing isotopes. But generally speaking, a closed system requirement is rarely fulfilled in natural condition. It is important then to evaluate any possible mechanisms which may cause the system an open one. Diffusion from groundwater in the aquifer to the adjacent aquitard is obviously one of such an important mechanism. If we know the hydraulic parameters of the aquifer and aquitards, and the initial input function of the radioactive tracers, we can calculate the tracer concentration from the solutions we derived in section 2. The apparent age can then be calculated by assuming a simple exponential decay from the initial concentration C_0 to the concentration value at a given point at given time which obeys the following equation:

$$t = -\frac{1}{\lambda}\ln(\frac{C}{C_0}) \qquad (4\text{-}48)$$

Notice that C/C_0 is our defined dimensionless concentration, so Eqs. (4-48) reduced to:

$$t = -\frac{1}{\lambda}\ln(C_D) \qquad (4\text{-}49)$$

The effects of different processes, such as radioactive decay, retardation, hydrodynamic dispersion and diffusion can be manifested by comparing the apparent age to true age.

We can follow this idea and redo all the plots we presented before. For example, we plot Figure 4-2A as percentage of error in apparent age t_{app} as $(t_{app} - t_{true})/t_{true} * 100\%$ against real age (t_{true}), which is shown as Figure 4-7. Figure 4-7 shows that the results of groundwater age dating based on radiometric measurement data can vary in wild range, with the most accurate dating window roughly about the time when the plume of radioactive tracer passes through the sampling point. One should always be cautious when interpreting and using radiometric age data.

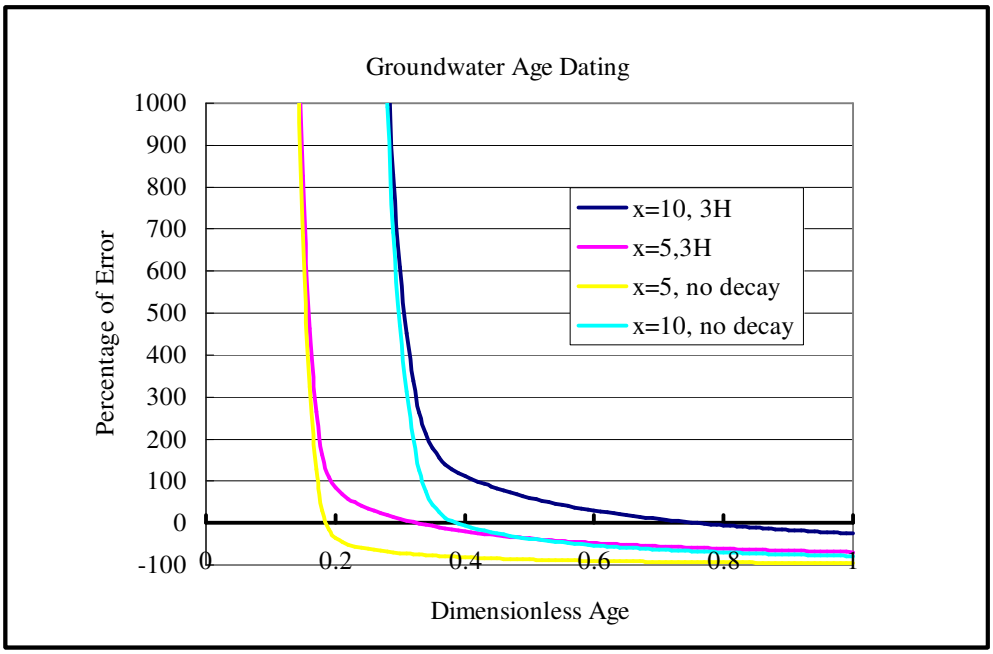

Figure 4-7. Plot of percentage of apparent age vs. absolute age.

4.5. Summary and Conclusions

This chapter presented our work on an analytical modeling of radioactive nuclides transport in an aquifer-aquitard system. The model can handle advection, dispersion, radioactive decay, retardation, and diffusion. This model cannot deal with mixing, in-situ production, and some other processes. Model can be useful to interpret radiometric groundwater age data, or using groundwater age distribution data to find out hydrologic parameters. The model can be easily extended to deal with radioactive isotopes transport in water table aquifer, providing that the vertical flow in the

unsaturated zone can be neglected. It can also extend to solve non radioactive environmental tracer transport in aquifer aquitard system, such as CFCs. In this case, we treat the biodegradation of CFCs as exponential decay.

Table 4-1: Default value of parameters used in Chapter IV.

Isotope	^{3}H
Decay constant	$\lambda = 1.786 * 10^{-9}\, s^{-1}$
Longitudinal dispersivity	$a_x = 1\text{m}$
Vertical dispersivity	$a_z = 0.1\text{m}$
Effective diffusion coefficient	$D_{01} = 1.18 * 10^{-9}\ m^2/s.$
Pore velocity in aquifer	$V = 1.16 \times 10^{-6}\ \text{m/s}$
Dimensionless x	*X=10*
Dimensionless z	*Z=0*
Thickness of aquifer	*2B=20m*
Retardation factor of the aquifer	*R = 1*
Retardation factor of the aquitard	$R_1 = 5$

Table 4-2: Definition of dimensionless terms used in Chapter IV.

Dimensionless Term	Definition	Dimensionless Term	Definition
Dimensionless horizontal coordinate	$x_D = \frac{x}{B}\sqrt{\frac{D_z}{D_x}}$	Dimensionless vertical coordinator	$z_D = \frac{z}{B}$
Dimensionless Time	$t_D = \frac{D_z}{RB^2}t$	Dimensionless Concentration	$C_D = \frac{C}{C_0}$
Dimensionless Concentration in Upper Aquitard	$C_{1D} = \frac{C_1}{C_0}$	Dimensionless Concentration in lower Aquitard	$C_{2D} = \frac{C_2}{C_0}$
Ratio of effective diffusion coefficient of the upper aquitard to vertical dispersion coefficient of the aquifer	$\beta_1 = \frac{D_{01}}{D_z}$	Ratio of effective diffusion coefficient of the lower aquitard to vertical dispersion coefficient of the aquifer	$\beta_2 = \frac{D_{02}}{D_z}$
Peclet Number	$\gamma = \frac{vB}{\sqrt{D_x D_z}}$	Dimensionless Radioactive decay constant	$\kappa = \frac{B^2 R\lambda}{D_z}$
Ratio of porosities of the upper aquitard to the aquifer	$\sigma_1 = \frac{\theta_1}{\theta}$	Ratio of porosities of the lower aquitard to the aquifer	$\sigma_2 = \frac{\theta_2}{\theta}$
Ratio of retardation factors of the upper aquitard to the aquifer	$\varepsilon_1 = \frac{R}{R_1}$	Ratio of retardation factors of the lower aquitard to the aquifer	$\varepsilon_2 = \frac{R}{R_2}$

CHAPTER V

SUMMARY AND FUTURE WORK

5.1. Summary

In this dissertation, we improved the theory on the solute transport in an aquifer aquitard system. Three main contributions are made by completing this work.

First contribution of this work is by introducing the multiple precision Stehfest method to hydrogeologists. As far as we know, no others have tried this method in the field of solute transport. Because of it is easy to program and use by the users, suitable for large groups of equations, and can virtually accomplish any required accuracies, this method should be a valuable mathematical tool for researchers.

Second contribution of this work is to provide a 2-D solution for solute transport in a divergent radial flow field. The solutions can virtually deal with any type of input functions, from instantaneous pulse injection, periodic injection, multi-step injection, to constant injection, from fully penetrating injection to partially penetrating injection. The solutions also took into account of many transport processes, such as advection, dispersion, retardation and radioactive decay. These solutions gave more accurate results of solute concentration along its flow path, no matter whether one looked at multilevel sampling data or thickness averaged sampling data. The versatility and accuracy of the solutions ensures they are suitable for many kinds of applications, such as interpretations of divergent tracer tests, estimation of different hydrological parameters, finding point sources of contamination and so on.

The last contribution of this work is from the modeling of radioactive isotope transport in an aquifer-aquitard system. Again we considered most, but not all, important processes which may change the concentration ratio of radioactive isotopes, so results from these solutions post another constraints on groundwater age dating techniques other than the simple piston flow model. Our results show that apparent radiometric ages based on piston flow model are way off from the real age, and so call for the caution of interpretation and use of radiometric age data without any other geological constraints.

By finishing up this dissertation, still a lot of problems closely related to these topics may be worked out. For example, in chapter IV, some other processes are also very important in terms of change the isotopic ratio, i. e. mixing of water from different sources, in situ generation of radiogenic isotopes, concentration change of the radiogenic isotopes, diffusion of old water from the aquitard to the aquifer and so on, given enough time, some of them can be incorporated into the 2-D model, so as to make the model more comprehensive. If we have already developed such a comprehensive model, it is possible to study the interactions between these different processes.

5.2. Future Work

As we can see from this dissertation, analytical modeling can provide deep insight understanding of the aquifer-aquitard system, but analytical modeling are limited to solve only very simple problems. Complex boundary and initial conditions will easily cause a problem analytically unsolvable. For example, in this work we focused on aquifer-aquitard systems, but how about clay lenses of variable size in the aquifer layers?

The small scale heterogeneity will cause the complex flow pattern even under steady state condition, and once the magnitude and direction of flow are changing from place to place, I cannot think about any chances to solve such a problem.

One of my current thoughts about my future work is to study solute transport using numerical model. With the sophisticated numerical tools available in the market, researchers now can have GIS (Geographic Information System) based groundwater modeling system such as GMS (Groundwater modeling System). The software package GMS has the ability to couple surface water and groundwater flow and transport processes. Also the fast development of computer hardware provides researchers better chances to run watershed or hillslope scale groundwater modeling in their personal computers. Ideally the complicated numerical model can be compared with simple analytical models, if both models are close to reality.

Another direction I like to pursue my future study on aquifer-aquitard system is to go to the real field. To solve real geo-environmental problems, collect real hydro-geological data, and then model the real system is my dream.

REFERENCES

Abramowitz, M. and Stegun, I.A., (1972), *Handbook of Mathematical Functions.* Dover Publications, New York.

Ball, W.P., Liu, C., Xia, G., and Young, D. F. (1997a), A diffusion-based interpretation of tetrachloroethene and trichloroethene concentration profiles in a groundwater aquitard, *Water Resour. Res.*, *33*(12), 2741-2757.

Ball, W.P., Xia, G., Durfee, D. P., Wilson, R. D., Brown, M. J., and Mackay, D. M. (1997b), Hot methanol extraction for the analysis of volatile organic chemicals in subsurface core samples from Dover Air Force Base, Delaware, *Ground Water Monitoring and Remediation*, *17* (1), 104-121.

Bear, J. (1972), *Dynamics of Fluids in Porous Media*, Elsevier, New York.

Bethke, C. M. and Johnson, T. M. (2002), Paradox of groundwater age: Correction. *Geology, 30*(4), 385-388.

Carslaw, H. and Jaeger, J. (1959). *Conduction of Heat in Solids.* Oxford University Press, Oxford.

Chen, C. S. (1985), Analytical and approximate solutions to radial dispersion from an injection well to a geological unit with simultaneous diffusion into adjacent strata, *Water Resour. Res.*, *21*(8), 1069-1076.

Chen, C. S. (1987), Analytical solutions for radial dispersion with Cauchy boundary at injection well, *Water Resour. Res., 23*(7), 1217-1224.

Cook, P. G., Solomon, D. K., Plummer, L, N., Busenberg, E. and Schiff, S. L. (1995) Chlorofluorocarbons as tracers of groundwater transport processes in a shallow, silty sand aquifer. *Water Resour. Res., 31*, 425-434.

de Hoog, F. R., Knight, J. H., and Stokes, A. N. (1982). An improved method for numerical inversion of Laplace transforms. *S.I.A.M. J. Sci. and Stat. Comput., 3*(3), 357-366.

Domenico, P.A., and Schwartz, F. W. (1998), *Physical and Chemical Hydrogeology* (2nd ed.), Wiley, New York.

Fetter, C.W. (1999), *Contaminant Hydrogeology* (2nd edition), Prentice-Hall, Upper Saddle River, NJ.

Freeze, R. A. and Cherry, J. A. (1979), *Groundwater,* Prentice-Hall, Upper Saddle River, NJ.

Freyberg, D. (1986), A natural gradient experiment of solute transport in a sand aquifer 2. Spatial moments and the advection and dispersion of nonreactive tracers. *Water Resour. Res., 22* (13), 2031-2046.

Frolov, G. A. and Kitaev, M. Y. (1998). Improvement of accuracy in numerical methods for inverting Laplace transforms based on the Post-Widder formula. *Computers & Mathematics with Applications, 36* (5), 23-34.

Fujikawa, Y., and Fukui, M. (1990), Adsorptive solute transport in fractured rock: Analytical solutions for delta-type source conditions, *J. Contam. Hydrol*., *6*(1), 85-102.

Gleick, P. H. (1993), *Water in Crisis-A guide to the World's Fresh Water Resources*, Oxford University Press, Oxford.

Goode, D. J. (1996). Direct simulation of groundwater age. *Water Resour. Res., 32*, 289-296.

Hendry, M.J., Ranville, J. R., Boldt-Leppin, B. E. J., and Wassenaar, L. I. (2003), Geochemical and transport properties of dissolved organic carbon in a clay-rich aquitard, *Water Resour. Res., 39*(7), 1194, doi: 10.1029/2002WR001943.

Hoopes, J. A. and D. R. F. Harleman (1967), Wastewater recharge and dispersion in porous media. *J. Hydr. Div. Proc. ASCE, 5*, 51-71.

Hsieh, P. A. (1986), A new formula for the analytical solution of the radial dispersion problem, *Water Resour. Res.*, *22*(11), 1597-1605.

Hubbard, S. S. and Y. Rubin (2000), Hydrogeological parameter estimation suing geophysical data: A review of selected techniques. *J. Contaminant Hydrology*, *45*, 3-34.

Hunkeler, D., Chollet, N., Pittet, X., Aravena, R., Cherry, J. A., and Parker, B. L. (2004), Effect of source variability and transport processes on carbon isotope ratios of TCE and PCE in two sandy aquifers, *J. Contam. Hydrol*., *74*(1-4), 265-282.

Jahne, B., Heinz, G. and Deitrich, W. (1987). Measurement of the diffusion coefficients of sparingly soluble gases in water. *Jour. Geophys. Res., 92,* 6614-6626.

Johnson, R. L., Cherry, J. A., and Pankow, J. F. (1989), Diffusive contaminant transport in natural clay: A field example and implications for clay-lined waste disposal sites, *Environmental Sci. and Technol.*, *23*, 340-49.

Lehmann, B. E., Love, A., Purtschert, R., Collon, R., Loosli, H. H., Kutschera, W., Beyerle, U., Aeschbach-Hertig, A., Moran, J., Tolstikhin, I. N. and Groning, M. (2003), A comparison of groundwater dating with ^{81}Kr, ^{36}Cl and ^{4}He in four wells of the Great Artesian Basin, Australia. *Earth and Planetary Science Letters, 211,* 237-250.

Liu, C.X., and Ball, W. P. (1999), Application of inverse methods to contaminant source identification from aquitard diffusion profiles at Dover AFB, Delaware, *Water Resour. Res.*, *35*(7), 1975-1985.

Liu, C.X., and Ball, W. P. (2002), Back diffusion of chlorinated solvent contaminants from a natural aquitard to a remediated aquifer under well-controlled field conditions: Predictions and measurements, *Ground Water*, *40*(2), 175-184.

Moench, A. F. (1991), Convergent radial dispersion: a note on evaluation of the Laplace transform solution, *Water Resour. Res., 27*(12), 3261-3264.

Moench, A. F., and Ogata, A. (1981), A numerical inversion of the Laplace transform solution to radial dispersion in a porous medium, *Water Resour. Res., 17*(1), 250-252.

Moreno, L., I. Neretnieks, and T. Eriksen (1985), Analysis of some laboratory tracer runs in natural fissures, *Water Resour. Res.*, *21*(7), 951-958.

Murli, A. and Rizzardi, M. (1990). Algorithm 682 Talbot's method for the Laplace transform inversion problem. *ACM Transactions on Mathematical Software, 16*(2), 158-168.

Neretnieks, I. (1980), Diffusion in the rock matrix: An important factor in radionuclide retardation?, *J. Geophys. Res.*, *85*(B8), 4379-4397.

Neretnieks, I., Eriksen, T., and Tähtinen, P. (1982), Tracer movement in a single fissure in granitic rock: Some experimental results and their interpretation, *Water Resour. Res.*, *18*(4), 849-858.

Parker B.L., Cherry, J. A., and Chapman, S. W. (2004), Field study of TCE diffusion profiles below DNAPL to assess aquitard integrity, *J. Contam. Hydrol*., *74*(1-4), 197-230.

Pinder, G. F. (2002), *Groundwater Modeling Using Geographical Information Systems*. John Wiley & Sons, Inc., New York.

Plummer, L, N., Busenberg, E., Drenkard, S., Schlosser, P., Ekwurzel, B., Weppernig, R., McConnell, J. B., and Michel, R. L. (1998), Flow of river water into a karstic limestone aquifer—2. Dating the young fraction in groundwater mixtures in the Upper Floridan aquifer near Valdosta, Georgia. *Applied Geochemistry, 13*(8), 1017-1043.

Ptak, T., Piepenbrink, M. and Martac, E. (2004), Tracer tests for the investigation of heterogeneous porous media and stochastic modeling of flow and transport – a review of some recent developments. *J. Hydrology*, *294,* 122-163.

Rasmuson, A., and Neretnieks, I. (1981), Migration of radionuclides in fissured rock: The influence of micropore diffusion and longitudinal dispersion, *J. Geophys. Res.*, *86*(B5), 3749-3758.

Starr, R. C., Gillham, R. W., and Sudicky, E. A. (1985), Experimental investigation of solute transport in stratified porous media, 2. The reactive case, *Water Resour. Res.*, *21*(7), 1043-1050.

Stehfest, H. (1972), Numerical inversion of Laplace transforms, *Commun. ACM, 13*(1), 47-49.

Sudicky, E. A., and Frind, E. O. (1981), Carbon 14 dating of groundwater in confined aquifers: Implication of aquitard diffusion *Water Resour. Res.*, *17*(4), 1060-1064.

Sudicky, E. A., and Frind, E. O. (1982), Contaminant transport in fractured porous media: Analytical solutions for a system of parallel fractures, *Water Resour. Res.*, *18*(6), 1634-1642.

Sudicky, E. A., and Frind, E. O. (1984), Contaminant transport in fractured porous media: Analytical solutions for a two-member decay chain in a single fracture, *Water Resour. Res.*, *20*(7), 1021-1029.

Sudicky, E. A., Gillham, R. W., and Frind, E. O. (1985), Experimental investigation of solute transport in stratified porous media, 1. The nonreactive case, *Water Resour. Res.*, *21*(7), 1035-1041.

Sun, D., and Zhan, H. (2006), Flow to a horizontal well in an aquifer-aquitard system, *Journal of Hydrology, 321*(1-4)*,* 364-376.

Szabo, Z., Rice, D. E., Plummer, L. N., Busenberg, E., Drenkard, S. and Schlosser, P. (1996), Age dating of shallow groundwater with chlorofluorocarbons, tritium/helium 3 and flow path analysis, southern New Jersey coastal plain. *Water Resour. Res., 32*(4), 1023-1038.

Talbot, A. (1979), The accurate numerical inversion of the Laplace transforms, *J. Inst. Math. Its Appl.*, *23,* 97-120.

Tang, D. H., Frind, E. O., and Sudicky, E. A. (1981), Contaminant transport in fractured porous media: Analytical solution for a single fracture, *Water Resour. Res.*, *17*(3), 555-564.

Tang, Y., and Aral, M. M. (1992a), Contaminant transport in layered porous media, 1. General solution, *Water Resour. Res.*, *28*(5), 1389-1397.

Tang, Y., and Aral, M. M. (1992b), Contaminant transport in layered porous media, 2. Applications, *Water Resour. Res.*, *28*(5), 1399-1406.

USEPA (U. S. Environmental Protection Agency). 1998. Report Brochure: National Water Quality Inventory: 1996 Report to Congress, Background Section. Washington, DC. Office of Water, (28 March 2000) [online] http:/www.epa.gov/OW/resources/brochure/broch2.html.

Valkó, P. P. and Abate, J. (2004), Comparison of sequence accelerators for the Gaver method of numerical Laplace transform inversion, *Computers and Mathematics with Applications, 48,* 629-636.

Valkó, P. P. and Vajda, S. (2002), Inversion of noise-free Laplace transforms: Towards a standardized set of test problems. *Inverse Problems in Engineering, 10*(5), 467-483.

Vengosh, A., Gill, J., Davisson, M. L. and Hudson, G. B. (2002). A multi-isotope (B, Sr, O, H, and Cl) and age dating (^{3}H - ^{3}He and ^{14}C) study of groundwater from Salinas Valley, California: Hydrochemistry, dynamics, and contamination processes. *Water Resour. Res., 38*(1), 1008, 10.1029/2001WR000517.

Wang, J. H., Robinson, C. V. and Edelman, E. S. (1952), Self-diffusion and structure of liquid water: III. Measurement of the self-diffusion of liquid water with ^{2}H, ^{3}H and ^{18}O as tracers. *J. Am. Chem. Soc.*, *75,* 466-470.

Young, D. F., and Ball, W. P. (1998), Estimating diffusion coefficients in low-permeability porous media using a macropore column, *Environmental Sci. and Technol., 32* (17), 2578-2584.

Zhan, H., Bian, A., and Sun, D. (2006), Two Dimensional solute transport in an aquifer-aquitard system. *Submitted to Water Resources Research.*

Zlotnik, V. A. and Zhan, H. B. (2005), Aquitard effect on drawdown in water table aquifer. *Water Resou. Res., 41,* W06022, doi: 10.1029/2004WR003716.

APPENDIX A

SOLUTE TRANSPORT IN AN AQUIFER BOUNDED BY IDENTICAL UPPER AND LOWER AQUITARDS

Considering the boundary condition of Eqs. (3-15), the following solution is proposed for $\overline{C}$:

$$\overline{C} = \sum_{n=0}^{\infty} A_n \overline{C}_r(r, p, n)\cos(\omega_n z), \tag{A-1}$$

where A_n is the coefficient that needs to be determined, $\overline{C}_r(r, p, n)$ is the part related to the r coordinate, and ω_n is the frequency of the Fourier transform along the z-axis. Substituting Eqs. (A-1) into (3-12) results in the following equation for $\overline{C}_x(x, p, n)$:

$$\frac{d^2\overline{C}_r}{dr^2} - \frac{d\overline{C}_r}{dr} - (\lambda + rp + k\omega_n^2)\overline{C}_r = 0. \tag{A-2}$$

Equation (A-2) can be transformed into standard form of Airy function (Eqs. (3-24)) by the follow steps:

$$\overline{C}_r = ye^{\frac{r}{2}}. \tag{A-3}$$

$$x = p^{-\frac{2}{3}}(\lambda + rp + k\omega_n^2 + \frac{1}{4}). \tag{A-4}$$

General solution of Airy function is:

$$y = d_1 Ai(x) + d_2 Bi(x) \tag{A-5}$$

d_1 and d_2 are two constants to be determined. Notice that $Bi(x)$ goes to infinity when x approaches infinity, so consider the boundary condition of Eqs. (3-14) will yield the general solution of (A-2):

$$\overline{C}_r(r,p,n) = d_1 e^{\frac{r}{2}} Ai\left[p^{-\frac{2}{3}}\left(\lambda + rp + k\omega_n^2 + \frac{1}{4}\right)\right]. \tag{A-6}$$

Therefore, the proposed solution for the aquifer becomes:

$$\overline{C} = \sum_{n=0}^{\infty} A_n e^{\frac{r}{2}} Ai\left[p^{-\frac{2}{3}}\left(\lambda + rp + k\omega_n^2 + \frac{1}{4}\right)\right]\cos(\omega_n z),\ 0 \le z \le 1 \tag{A-7}$$

The solution to Eqs. (3-16) with the boundary conditions of (3-17) and (3-19) is:

$$\overline{C}_1 = \overline{C}_1(r, z=1, p)\exp\left[\sqrt{k_3 + k_1 p}\,(1-z)\right] = \overline{C}(r, z=1, p)\exp\left[\sqrt{k_3 + k_1 p}\,(1-z)\right]. \tag{A-8}$$

Substituting Eqs. (A-7) into (3-18) and considering (A-8) will lead to:

$$\omega_n \tan(\omega_n) = k_2 r\sqrt{k_3 + k_1 p}\,. \tag{A-9}$$

For any given r and p, ω_n can be determined from (A-9). Once ω_n has been determined, one can find A_n from the boundary condition (3-13). Substituting (A-7) into (3-13) leads to:

$$F(z,p) = \sum_{n=0}^{\infty} A_n e^{\frac{r_0}{2}} Ai\left[p^{-\frac{2}{3}}\left(\lambda + r_0 p + k\omega_n^2 + \frac{1}{4}\right)\right]\cos(\omega_n z)\,. \tag{A-10}$$

Conducting inverse Fourier transform of (A-10) results in:

$$A_n = \frac{G(F,p,\omega_n)}{A(r_0,p,\omega_n)} \tag{A-11}$$

where $G(F,p,\omega_n)$ and $A(r_0,p,\omega_n)$ are defined in (3-22) and (3-23).

Therefore, $\overline{C}$ and $\overline{C}_1$ are derived after substituting (A-11) into (A-7) and (A-8).

APPENDIX B

SOLUTE TRANSPORT IN AN AQUIFER BOUNDED BY DIFFERENT UPPER AND LOWER AQUITARDS

The differences between the upper and lower aquitard may expressed as different effective molecular diffusion coefficients and/or different porosities. Now the aquifer is bounded from top and bottom by different aquitards. Continuity of concentration and vertical flux along both upper and lower aquifer-aquitard boundary requires:

$$\overline{C}_1(r, z=1, p) = \overline{C}(r, z=1, p), \tag{B-1}$$

$$\frac{\partial \overline{C}_1(r, z=1, p)}{\partial z} = \frac{1}{k_{2u}} \frac{1}{r} \frac{\partial \overline{C}(r, z=1, p)}{\partial z}, \tag{B-2}$$

$$\overline{C}_2(r, z=0, p) = \overline{C}(r, z=0, p), \tag{B-3}$$

$$\frac{\partial \overline{C}_2(r, z=0, p)}{\partial z} = \frac{1}{k_{2l}} \frac{1}{r} \frac{\partial \overline{C}(r, z=0, p)}{\partial z}, \tag{B-4}$$

The proposed new solution for $\overline{C}$ reads:

$$\overline{C} = \sum_{n=0}^{\infty} A_n \overline{C}_r(r, p, n) \cos(\omega_n z + \mu_n). \tag{B-5}$$

Notice that (B-5) is different from (A-1) by including an additional phase term in the cosine function. $\mu_n = 0$ if the bottom boundary is no vertical flux boundary. In this special case, the solution will collapse to the same as discussed in previous section. Using similar procedures as described in APPENDIX A, one can obtain

$$\overline{C} = \sum_{n=0}^{\infty} A_n e^{\frac{r}{2}} Ai\left[p^{-\frac{2}{3}} \left(\lambda + rp + k\omega_n^2 + \frac{1}{4} \right) \right] \cos(\omega_n z + \mu_n),\ 0 \le z \le 1. \tag{B-6}$$

$$\overline{C_1} = \sum_{n=0}^{\infty} A_n e^{\frac{r}{2}} Ai\left[p^{-\frac{2}{3}}\left(\lambda + rp + k\omega_n^2 + \frac{1}{4}\right)\right]\cos(\omega_n + \mu_n)\exp\left[\sqrt{k_{3u} + k_{1u} p}\,(1-z)\right] \quad ,$$

$1 \le z \le \infty$. (B-7)

$$\overline{C_2} = \sum_{n=0}^{\infty} A_n e^{\frac{r}{2}} Ai\left[p^{-\frac{2}{3}}\left(\lambda + rp + k\omega_n^2 + \frac{1}{4}\right)\right]\cos(\mu_n)\exp\left[\sqrt{k_{3l} + k_{1l} p}\, z\right], \; -\infty \le z \le 0 . \quad \text{(B-8)}$$

Substituting (B-1), (B-6) and (B-7) into (B-2) results in:

$$\omega_n \tan(\omega_n + \mu_n) = r k_{2u}\sqrt{k_{3u} + k_{1u} p}\,, \quad \text{(B-9)}$$

Similarly substituting (B-3), (B-6) and (B-8) into (B-4) results in:

$$-\omega_n \tan(\mu_n) = r k_{2l}\sqrt{k_{3l} + k_{1l} p}\,. \quad \text{(B-10)}$$

Expending $\tan(\omega_n + \mu_n)$ to $\tan(\omega_n)$ and $\tan(\mu_n)$ and considering the second equation in (B-6) will lead to:

$$\tan(\omega_n) = \frac{\omega_n r k_{2u}\sqrt{k_{3u} + k_{1u} p} + r k_{2l}\sqrt{k_{3l} + k_{1l} p}}{\left(\omega_n^2 - r^2 k_{2u} k_{2l}\sqrt{k_{3u} + k_{1u} p}\sqrt{k_{3l} + k_{1l} p}\right)}. \quad \text{(B-11)}$$

After determining ω_n from (B-11), μ_n is calculated from (B-9)

$$\mu_n = -\tan^{-1}\left[r k_{2l}\sqrt{k_{3l} + k_{1l} p}\,/\,\omega_n\right]. \quad \text{(B-12)}$$

The coefficient A_n is obtained by substituting (B-6) into (3-13):

$$F(z,p) = \sum_{n=0}^{\infty} A_n e^{\frac{r_0}{2}} Ai\left[p^{-\frac{2}{3}}\left(\lambda + r_0 p + k\omega_n^2 + \frac{1}{4}\right)\right]\cos(\omega_n z + \mu_n)\,. \quad \text{(B-13)}$$

Conducting inverse Fourier transform of (A-10) results in:

$$A_n = \frac{G(F, p, \omega_n, \mu_n)}{A(r_0, p, \omega_n)} \quad \text{(B-14)}$$

where $G(F, p, \omega_n, \mu_n)$ and $A(r_0, p, \omega_n)$ are defined in (3-33) and (3-23).

Substituting A_n into (B-6) - (B-8) will result in the solutions for $\overline{C}$, $\overline{C_1}$, and $\overline{C_2}$.

APPENDIX C

SOLUTE TRANSPORT IN AN AQUIFER BOUNDED BY IDENTICAL UPPER AND LOWER AQUITARDS

Considering the boundary condition of Eqs. (4-15), the following solution is proposed for $\overline{C}$:

$$\overline{C} = \sum_{n=0}^{\infty} A_n \overline{C}_x(x, p, n)\cos(\omega_n z)\,, \tag{C-1}$$

where A_n is the coefficient that needs to be determined, $\overline{C}_x(x, p, n)$ is the part related to the x coordinate, and ω_n is the frequency of the Fourier transform along the z-axis. Substituting Eqs. (C-1) into (4-12) results in the following equation for $\overline{C}_x(x, p, n)$:

$$\frac{d^2\overline{C}_x}{dx^2} - \gamma\frac{d\overline{C}_x}{dx} - (p + \kappa + \omega_n^2)\overline{C}_x = 0\,. \tag{C-2}$$

Considering the boundary condition of (4-14) will yield the general solution of (C-2):

$$\overline{C}_x(x, p, n) = \exp\left[\left(\gamma - \sqrt{\gamma^2 + 4(p + \kappa + \omega_n^2)}\right)\frac{x}{2}\right]. \tag{C-3}$$

Therefore, the proposed solution for the aquifer becomes:

$$\overline{C} = \sum_{n=0}^{\infty} A_n \exp\left[\left(\gamma - \sqrt{\gamma^2 + 4(p + \kappa + \omega_n^2)}\right)\frac{x}{2}\right]\cos(\omega_n z)\,,\ 0 \le z \le 1 \tag{C-4}$$

The solution to Eqs. (4-16) with the boundary conditions of (4-17) and (4-19) is:

$$\overline{C}_1 = \overline{C}_1(x, z = 1, p)\exp\left[\sqrt{\frac{p + \kappa}{\varepsilon_1\beta_1}}(1 - z)\right] = \overline{C}(x, z = 1, p)\exp\left[\sqrt{\frac{p + \kappa}{\varepsilon_1\beta_1}}(1 - z)\right]. \tag{C-5}$$

Substituting Eqs. (C-4) into (4-18) and considering (C-5) will lead to:

$$\omega_n \sin(\omega_n) = \sigma_1 \sqrt{\frac{\beta_1}{\varepsilon_1}(p+\kappa)} \cos(\omega_n), \text{ or } \omega_n \tan(\omega_n) = \sigma_1 \sqrt{\frac{\beta_1}{\varepsilon_1}(p+\kappa)}. \quad \text{(C-6)}$$

After determining ω_n from (C-6), one can determine A_n from the boundary condition (4-13). Substituting (C-5) into (4-13) leads to:

$$\sum_{n=0}^{\infty} A_n \cos(\omega_n z) = 1. \quad \text{(C-7)}$$

Conducting inverse Fourier transform of (C-7) results in:

$$A_n = \frac{4\sin(\omega_n)}{F(\omega_n)}, \text{ where } F(\omega_n) = \sin(2\omega_n) + 2\omega_n. \quad \text{(C-8)}$$

Therefore, $\overline{C}$ and $\overline{C}_1$ are derived after substituting (C-8) into (C-4) and (C-5).

APPENDIX D

SOLUTE TRANSPORT IN AN AQUIFER BOUNDED BY DIFFERENT UPPER AND LOWER AQUITARDS

If the upper and lower aquitards have different effective molecular diffusion coefficients and porosities, continuity of mass flux at the upper and lower boundaries of the aquifer (Eqs. (4-18) and (4-30) respectively) will result in the following dimensionless forms in Laplace domain:

$$\left.\frac{\partial \overline{C}}{\partial z}\right|_{z=1} = \beta_1\sigma_1 \left.\frac{\partial \overline{C}_1}{\partial z}\right|_{z=1}, \quad \left.\frac{\partial \overline{C}}{\partial z}\right|_{z=0} = \beta_2\sigma_2 \left.\frac{\partial \overline{C}_2}{\partial z}\right|_{z=0}. \tag{D-1}$$

The proposed new solution for $\overline{C}$ becomes

$$\overline{C} = \sum_{n=0}^{\infty} A_n \overline{C}_x(x,p,n)\cos(\omega_n z + \mu_n). \tag{D-15}$$

Notice that the difference between (D-2) and (C-1) is the inclusion of a phase term in the cosine function. In general, $\mu_n \neq 0$ for the diffusive upper and lower boundaries. $\mu_n = 0$ is the case when the low boundary is no mass flux bottom, such as those in Section 4.2.2 and 4.2.3. In other words, the problems discussed in section 4.2.2 and 4.2.3 are two special cases of this general problem. Using similar procedures as described in APPENDIX C, one can obtain

$$\overline{C} = \sum_{n=0}^{\infty} A_n \exp\left[\left(\frac{\gamma - \sqrt{\gamma^2 + 4(p+\kappa+\omega_n^2)}}{2}\right)x\right]\cos(\omega_n z + \mu_n), \quad 0 \le z \le 1. \tag{D-3}$$

$$\overline{C}_1 = \sum_{n=0}^{\infty} A_n \exp\left[\left(\frac{\gamma - \sqrt{\gamma^2 + 4(p+\kappa+\omega_n^2)}}{2}\right)x\right]\cos(\omega_n + \mu_n)\exp\left[\sqrt{\frac{\kappa+p}{\varepsilon_1\beta_1}}(1-z)\right], \quad 1 \le z \le \infty. \tag{D-4}$$

$$\bar{C}_2 = \sum_{n=0}^{\infty} A_n \exp\left[\left(\frac{\gamma - \sqrt{\gamma^2 + 4(p+\kappa+\omega_n^2)}}{2}\right) x \right] \cos(\mu_n) \exp\left[\sqrt{\frac{\kappa+p}{\varepsilon_2 \beta_2}}\, z \right],\ -\infty \le z \le 0 . \tag{D-5}$$

Substituting (D-3)-(D-5) into (D-2) results in

$$\omega_n \tan(\omega_n + \mu_n) = \sigma_1 \sqrt{\beta_1 \left(\frac{\kappa+p}{\varepsilon_1}\right)}\ ,\ -\omega_n \tan(\mu_n) = \sigma_2 \sqrt{\beta_2 \left(\frac{\kappa+p}{\varepsilon_2}\right)} . \tag{D-6}$$

Expending $\tan(\omega_n + \mu_n)$ to $\tan(\omega_n)$ and $\tan(\mu_n)$ and considering the second equation in (D-6) will lead to:

$$\left(\omega_n^2 - \sigma_1 \sigma_2 (\kappa + p) \sqrt{\frac{\beta_1 \beta_2}{\varepsilon_1 \varepsilon_2}} \right) \tan(\omega_n) = \omega_n \sigma_1 \sqrt{\beta_1 \left(\frac{\kappa+p}{\varepsilon_1}\right)} + \sigma_2 \sqrt{\beta_2 \left(\frac{\kappa+p}{\varepsilon_2}\right)} . \tag{D-7}$$

After determining ω_n from (D-7), μ_n is calculated as (see (D-6))

$$\mu_n = -\tan^{-1}\left[\sigma_2 \sqrt{\beta_2 \left(\frac{\kappa+p}{\varepsilon_2}\right)} / \omega_n \right]. \tag{D-8}$$

The coefficient A_n is obtained using the first-type boundary condition at x=0 as

$$A_n = \frac{4 F_1(\omega_n, \mu_n)}{F_2(\omega_n, \mu_n)}, \tag{D-9}$$

where

$$F_1(\omega_n, \mu_n) = \sin(\omega_n + \mu_n) - \sin(\mu_n)\ ,\ F_2(\omega_n, \mu_n) = 2\omega_n + \sin(2\omega_n + 2\mu_n) - \sin(2\mu_n) . \tag{D-10}$$

Substituting A_n into (D-3) - (D-5) will result in the solutions for $\bar{C}$, $\bar{C}_1$, and $\bar{C}_2$.

VITA

Aiguo Bian
Visiting Assistant Professor
Department of Physics and Geosciences, Texas A&M University-Kingsville
MSC 175, 700 University BLVD, Kingsville, TX 78363
Office: (361)-593-2261; Cell: (979)-422-3373
Aiguo.bian@gmail.com

EDUCATION:

Ph.D. Geology, Texas A&M University, College Station, TX, (GPA 4.0/4.0). May 2007.

B.S. Structural Geology, Beijing University, GPA: 3.5/4.0, July 1996.

WORK HISTORY:

Sept 1996- Aug 2000: Research Assistant, Institute of Geology, Chinese Academy of Sciences (IGCAS). Mainly worked with Prof. Zhai Mingguo on a project of evaluation of mineral resources of Northern China.

Sept 2000- Aug 2002: Research Assistant or Teaching Assistant, Department of Geology and Environmental Sciences, Stanford University. Teaching mineralogy and metamorphic rock labs, and worked with Prof. J. G. Liou on ultrahigh pressure metamorphic rocks in the Central China Collision Zone.

Sept 2002- May 2006: Teaching Assistant, Department of Geology and Geophysics, Texas A&M University, College Station. Teaching physical geology labs and working with Prof. Hongbin Zhan on solute transport in aquifer-aquitard system.

Sept 2006-May 2007: Visiting Assistant Professor, Department of Physics and Geosciences, Texas A&M University-Kingsville, teaching the following courses: earth sciences I and II, structural geology, environment geology, and engineering geology.

PUBLICATIONS:

Zhan. H and Bian, A., 2006, A method of calculating pumping induced leakage, *Journal of Hydrology, 328,* 659-667.

Zhan, H., Bian, A., and Sun, D. (2006), Two dimensional solute transport in an aquifer-aquitard system. Submitted to *Water Resources Research.*